LAPPEENRANTA-LAHTI UNIVERSITY OF TECHNOLOGY LUT
School of Energy Systems
Mechanical Engineering

Alnecino Alves Netto

OPTIMIZATION OF GAS METAL ARC WELDING PROCESS PARAMETERS IN ULTRA-HIGH STRENGTH STEELS BASED ON PREDICTION

Examiner: D. Sc. (Tech.), docent Harri Eskelinen

ABSTRACT

Lappeenranta-Lahti University of Technology
School of Energy Systems
Degree Programme in Mechanical Engineering

Alnecino Francisco Alves Netto

Optimization of Gas Metal Arc Welding Process Parameters in Ultra High-Strength Steels Based on Prediction

Master's thesis
2019
70 pages, 33 figures, 9 tables and 1 appendix
Examiner: D. Sc. (Tech.), docent Harri Eskelinen

Keywords: Ultra-high strength steels, gas metal arc welding, heat input, welding simulation.

The search for materials to manufacture products with the aim of reduction weight and higher strength has been carried out during many years for many companies to fulfill requirements of lighter and safer products. The ultra-high strength steel (UHSS) is a complex and sophisticated material that came to be possible to develop products with properties that allows reduction of weight with increased strength due to the properties of the material, assisting for example, the automotive industry to save fuel of the vehicles and decreasing its emission. The gas metal arc welding (GMAW) has been used in several applications based on UHSS and may be considered as a well-established welding process. The welding of UHSS has a high level of complexity, mainly due to the higher quantity of alloys and the heat treatments applied to the material, which result in a microstructure with a higher sensitivity to the welding. The main purpose of the current thesis is to select the best parameters of GMAW to welding the S960 material based on prediction methods. To achieve the expected results, it was used finite element analysis (FEA) to simulate and evaluate the results comparing with experimental results obtained by welding a butt weld joint. The purpose of the use of a computational method is to approximate to the real condition and evaluate different structural and thermal behaviors. As a result, was found that the welding parameters and consequently the heat input derived from it has a great effect on the UHSS microstructure. The GMAW welding process achieved satisfactory results to weld the material and thickness analyzed, however, it was observed that some features such as pulse and laser welding along a specific joint shape must be considered to minimize the effect of heat input. By using FEA it was possible to estimate the extension of the heat affected zone (HAZ), the peak temperature and even the effect of the distortion and shrinkage. Those results are useful to predict a desirable behavior, or a microstructure based only on changes on the welding parameters. At last, could be observed that the new generation of UHSS achieved results with excellence on welded structures, though the number of grades is still a challenge that requires early analysis in order to obtain a prediction even closer to the real condition.

ACKNOWLEDGEMENTS

I want to express my sincere gratitude and respect to Dr. Paul Kah, who have suggested me this amazing subject which drive me to understand the relevance of this topic along his admirable knowledge and comprehension. In addition, I also want to thank Harri Eskelinen by support me during my final step of this thesis and to share so much experience is his classes along your rare mixture of friendly and so polite manner to teach. I would also like to thank Esa Hiltunen to provide me the necessary and relevant information from LUT welding laboratory to be used in this research.

I similarly would like to thank all my colleagues from LUT and say that it was an incredible experience to know too many friends from different nationalities in this special and inspiring environment that is LUT. Special thanks to Javier Hernandez!

Gostaria de agradecer a minha esposa Bárbara, que me amparou durante os momentos que tive dúvida se deveria ou não continuar e que muitas vezes fez o papel de pai para o nosso filho na minha ausência, para que eu pudesse me dedicar a este sonho que hoje se realiza. Ao meu filho, Benjamin, que me deu o incentivo para que eu entregasse sempre o melhor de mim, e para que eu seja o reflexo positivo que ele possa um dia se espelhar. Ao meu irmão, Thiago, que me apoiou desde o primeiro momento em que iniciei esta jornada e que sempre me confortou em saber que com ele eu poderia contar.

Gostaria também de dar agradecimentos mais que especiais à minha mãe, Maria Aparecida, que além de SEMPRE me apoiar em todas as minhas decisões, mostrou o quão essencial é para toda a família pela sua força e dedicação. Por último e não menos imporante, gostaria de agradecer e dedicar essa conquista ao meu pai, Jesus Francisco Alves (*in memoriam*), pelo exemplo de integridade e bom caráter, sempre me mostrando o caminho certo que eu deveria seguir e a importância que o estudo faria - e fez - na minha vida. Nunca iremos te esquecer!

Alnecino F. Alves Netto

Lappeenranta 18.11.2019

TABLE OF CONTENTS

LIST OF SYMBOLS AND ABBREVIATIONS

E	Arc voltage [V]
I	*C*urrent [A]
η	Arc welding efficiency [%]
Q	Energy input [kJ/mm]
q	Heat flux [W/mm²]
$t_{8/5}$	Cooling time from 800 to 500 ºC [s]
v	Welding speed [mm/min]
t	Time

3D	Three-dimensional
AHSS	Advanced high-strength steel
A-UHSS	Advanced ultra-high strength steel
AUST SS	Austenitic stainless steel
BH	Bake hardenable
BIW	Body-in-white
BM	Base material
CAD	Computer-aided design
CAE	Computer-aided engineering
CAx	Computer-aided technologies
CCT	Continuous cooling transformation
CE	Carbon equivalent
CGHAZ	Coarse grain heat affected zone
C-Mn	Carbon-manganese
CP	Complex-phase
CS	Commercial steel
DDS	Deep drawing steel
DP	Dual-phase
DS	Drawing steel
FB	Ferritic bainitic
FEA	Finite element analysis

FGHAZ	Fine grain heat affected zone
FZ	Fusion zone
GHG	Greenhouse gas
GMAW	Gas metal arc welding
HAZ	Heat-affected zone
HF	Hot formed
HHE	High hole expansion
HSLA	High strength low alloy
HSS	High strength steel
HV	Hardness Vickers
IF	Interstitial free
IIW	International Institute of Welding
IS	Isotropic
L-IP	Lighweight-induced plasticity
MART	Martensitic
MS	Martensitic steel
PHS	Press hardened steels
QC	Quenched and cold formed
S960	Structural steel with 960 MPa as minimum yield strength
SFHS	Stretch flanging high-strength
TRIP	Transformation induced plasticity
TWIP	Twinning induced plasticity
UHSS	Ultra high-strength steel
UTS	Ultimate tensile strength
VHSS	Very high strength steel
YS	Yield strength

LIST OF FIGURES

LIST OF TABLES

1 INTRODUCTION

The utilization of ultra-high strength steels (UHSS) and advanced high strength steels (AHSS) has increased and spread in a wide range of applications, mostly due to the advantages that these materials bring. In this chapter, will be presented a contextual information related to the classification of these materials and the necessities existed around its utilization in welding. Besides, the research problem, research questions, aims and methods of the present study will be clarified.

1.1 Background

The first indication related to a possible oil emergency occurred in 1975. Thus, the necessity to reduce fuel consumption started new aims to automotive companies which needed to decrease the weight of their vehicles. Along with the years, the fuel consumption reduction goal has become more intensive and reached different areas, changing the ways to design new products thinking in how to prevent the excessive weight and keep the desired properties of the materials. Additionally, due to environmental issues, there is also the necessity to decrease the gas emission generated by the fuel consumption and reduce the energy utilized to produce materials, assuring a more sustainable environment. (Fonstein 2015, p. 1; Alriksson & Henningsson 2015, p. 645.)

The AHSS/UHSS is an alternative to the fuel consumption reduction, that brings new perceptions and results, providing a weight reduction from 20% to 30% in passenger cars. In this case, the AHSSs are mostly applied in body-in-white (BIW) structure of vehicles, which steels sheets are joined by welding. Thus, reducing the weight of each vehicle in 10%, the fuel consumption may decrease from 3% to 7%, which are excellent results to use a material that also improve the safety and performance of passenger cars. (Mohrbacher, Spöttl & Paegle 2015, p. 5; Van Rensselar 2011, p. 39.)

The AHSS has been developed throughout many years, enabling nowadays the production of steels sheets which brings many benefits in comparison to others lightweight materials. However, to reach the current high-strength steels level in a range of 500 to 1700 MPa with improved ductility, it was necessary to consider different methods during its production.

Thus, changes in the microstructure by steel strengthening approaches, addition of alloys and micro alloys elements and heat treatment are the most used methods to achieve excellent results of AHSS. In this way, many grades and classification were created, allowing different combinations to a wide number of applications. (Fonstein 2015, p. 6; Demeri 2013, p. 20.)

Currently, the development of AHSS is in your third generation and the physical and metallurgical properties of the steel has changed until this point, affecting characteristics as thermal conductivity, hardenability, among others in usual welding processes. According to Mohrbacher, Spöttl & Paegle (2015, p. 5), in some manufacturing process (including welding) the improvement of materials has an essential role, affecting mostly properties as hardness and weldability that needs to be enhanced. Accordingly, the chemical composition and microstructure of the steel are some of the main issues that need to be considered when a material is modified.

In order to evaluate mechanical properties in dual-phase (DP) steels through gas metal arc welding (GMAW), Ramazani et al. (2014, p. 1) also mentioned the influence of heat input of welding process in the microstructure of the materials. The increase of the heat input and the gradient of the temperature changes the mechanical properties of DP steels. Furthermore, due to the higher heat input of GMAW process and its lower cooling rates, changes in the microstructure of the material may occur.

The development of new grades of AHSS and UHSS with different characteristics are studied and evaluated to enable its utilization in welding processes. In a study related to ultra-narrow gap laser and GMAW process accomplished by Guo et al. (2017, pp. 1-2), the S960 (structural steel with 960 MPa as minimum yield strength) developed by Tata Steels was analyzed. The S960 is a new steel that has excellent benefits as good impact toughness, weldability and formability, besides of its elevated strength, which make this material be a good option to application as heavy crane and others similar. The S960 is a high-strength low alloy (HSLA) wherein arc welding processes are normally used, however, the softening of the heat-affected zone (HAZ) is a typical issue in this welding process. The thermo-mechanical material properties of S960 using the GMAW process was also analyzed in another study accomplished by Bhatti et al. (2015, p. 879). In addition, it was also used the

finite element analysis (FEA) in order to evaluate welding process parameters and its influence in the results.

The selection of the AHSS/UHSS in welding applications requires a detailed evaluation relating all possible benefits and disadvantages. As mentioned previously, the possibility to reduce the material volume without compromise the safety and quality of the welded structure are essential factors in the selection of AHSS/UHSS. However, the welding parameters may need to be optimized to guarantee a reliable final product.

In this thesis, a UHSS S960 material welded by GMAW process was investigated trough welding simulation by finite element analysis. A three-dimensional (3D) model was generated during the welding simulation along welding modelling. Thus, due to the limited researches found related to the UHSS S960, the effect of heat input, microstructure and mechanical properties in GMAW was analyzed. To validate the finite element model, experimental results were used as input and a comparison between virtual and physical model was accomplished. The effects of the heat input in the microstructure were examined to evaluate the weldability in order to properly optimize the parameters of the welding process.

1.2 Research problem

The AHSS has been used in many different applications and processes such as the GMAW, where the selection of the welding parameters has an important impact on the final welding. Thus, the research problem focuses in some of the main problems in welding UHSS materials, that is based on the properly choice of welding parameters to achieve a high quality and consequently a reliable weld. The questions raised on welding UHSS is mostly related to the sensitivity of the material due the high number of alloys elements. Currently, there are a wide range and types of AHSS and UHSS, however, due to the differences of welding conditions and chemical composition of each grade, the same welding parameters may not be applicable to others grades of the material. Additionally, different methods of heat treatment used to ensure the properties of each grade of the UHSS may also provide difficulties in the welding process.

1.3 Research questions

The research questions covered in the present thesis are based on the following four main issues:

1. How to select properly the best parameters to weld UHSS materials with GMAW process?
2. What is necessary to accomplish a high quality and reliable welding using UHSS?
3. Why to choose UHSS as a material of a welded structure?
4. Which are the challenges of predicting GMAW process?

The items 1 and 2 above can be considered as the main research questions. Thus, the hypothesis raised suggest that the amount of heat input along with the chemical composition of the material is quite significant to determine the quality and performance of an UHSS welded structure, mainly due the sensitivity of the material. In this way, the parameters of GMAW process needed to be evaluated to predict the behavior of a welded structure.

1.4 Motivation

The current thesis is mainly motivated by the increase of AHSS and UHSS utilization and the encouragement in the use of these materials in welded structures due to the benefits brought. The advantages that UHSS welded structures offers may range since an elevated higher strength if compared to others steel grades until the possibility of weight reduction. Due to the necessity of greenhouse gas (GHG) reduction, many automotive companies are using UHSS as an alternative to reduce the weight of the vehicles and consequently reduce the fuel consumption. Additionally, the energy wasted to produce the materials is minimized due to the less material used to manufacturing the same structure.

The figure 1 shows a graph of AHSS and UHSS forecast utilization in North American light vehicles, which presents an average weight of AHSS and UHSS by vehicle. As can be seen, the average of the material used in the vehicle by weight in 2012 was 205 pounds (approximately 93 Kg) and in 2025 the expected quantity is 483 pounds (approximately 219 Kg), which corresponds to an increase of approximately 135%. In fact, the graph represents only a small portion of all applications where UHSS is being used. However, it helps to understand and analyze the evolution in the use of materials that can reduce weight and the

material usage, keeping the same strength – or even higher – and consequently helping the environment.

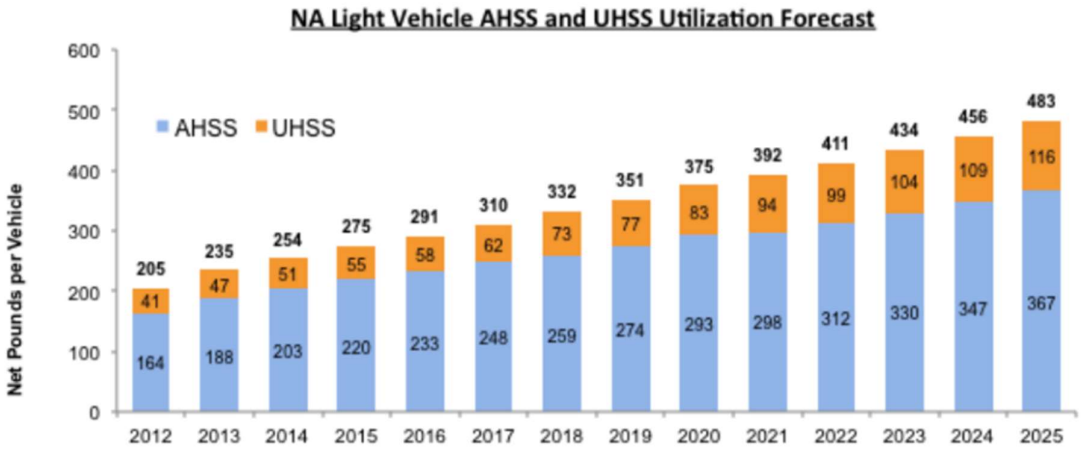

Figure 1. AHSS and UHSS utilization forecast in North American light vehicle (Abraham 2015, p. 18).

Furthermore, during the development of a product, it is essential to evaluate and consider not only the material cost, but also the structural performance and lifetime. It means that a final product is a sum of several stages that involves not only the material cost, but also design, assembly, among others. If a new proposed material is more expensive that the current, it is necessary to evaluate aspects as the durability and manufacturability. That is, overall costs involved with a new expensive material, which may lead to a lower cost if the performance and the manufacturing is considering. (Demeri 2013, p. 10.) This consideration is crucial when an AHSS is chosen, mostly due its higher cost if compared to ordinary materials as mild steels, however, the advantages of AHSS makes the choice feasible.

The researches involved in AHSSs are not only related to welding car body parts, but also to improve the general welding practices that includes essential parameters of the welding process. The AHSSs is a material that is in its third generation and many studies that involves welding effects has been developed along with the evolution of new grades of AHSS, comprising important mechanical properties, focusing in essential properties such as strength and toughness. (Májlinger, Kalácska & Spena 2016, pp. 615-616.)

In this way, the constant development of AHSS is also a motivation to accomplish a research on this material, since there is a lack of information in GMAW using the UHSS S960 material during the development of the current thesis. At last, the necessity to optimize the UHSS welded structures through prediction of the welding parameters in GMAW is an alternative to obtain better quality welds, prevent possible failures and contribute with the continuous use and development of AHSS and UHSS.

1.5 Objective

This research has the objective to identify alternative factors, control means and welding practices to optimize welding parameters to achieve a higher quality and reliability of welded structures. Therefore, to achieve the proposed goal, the ultra-high-strength steel S960 and the GMAW process will be studied. To accomplish this, it will be mostly considered and analyzed the issues related to the material, such as properties, applicability and weldability.

1.6 Research method

The research method used in this research consists of literature review, experimental tests and simulation by FEA. The validation of the results will be facilitated using the triangulation method. The utilization of this method aiming to ensure the verification using more than one approach, combining different ways to obtain the results. Thus, the literature review is mostly based in scientific articles and books found in databases offered by the library at Lappeenranta University of Technology. Using keywords related to the topic of the current research, many articles and books was analyzed to have the necessary knowledge to develop a physical system that will be used in further steps.

The results of experimental tests are related of some tests accomplished on the welding laboratory of the Lappeenranta University of Technology. The tests used the same material of this research, providing the material specification and other information relating to the welding conditions. The information of this results was used as initial input to the experimental design.

Furthermore, simulations based on FEA will be designed and accomplished to achieve results approaching to the real welding conditions of the GMAW process. Additionally, the

material properties of AHSS will also be applied along a welding feature tool provided by the FEA software.

1.7 Organization of the study

As can be seen by the figure 2, the research outline is divided in 8 steps. Initially the research problem was stipulated due a necessity to find optimum welding parameters based on prediction to provide suitable welds using the proposed AHSSs material. The second step has the role to deepen knowledge into the material and welding process selected on the researches available. With the necessary knowledge, the hypothesis of what may affect the research questions was formulated to start the design of the experimental design.

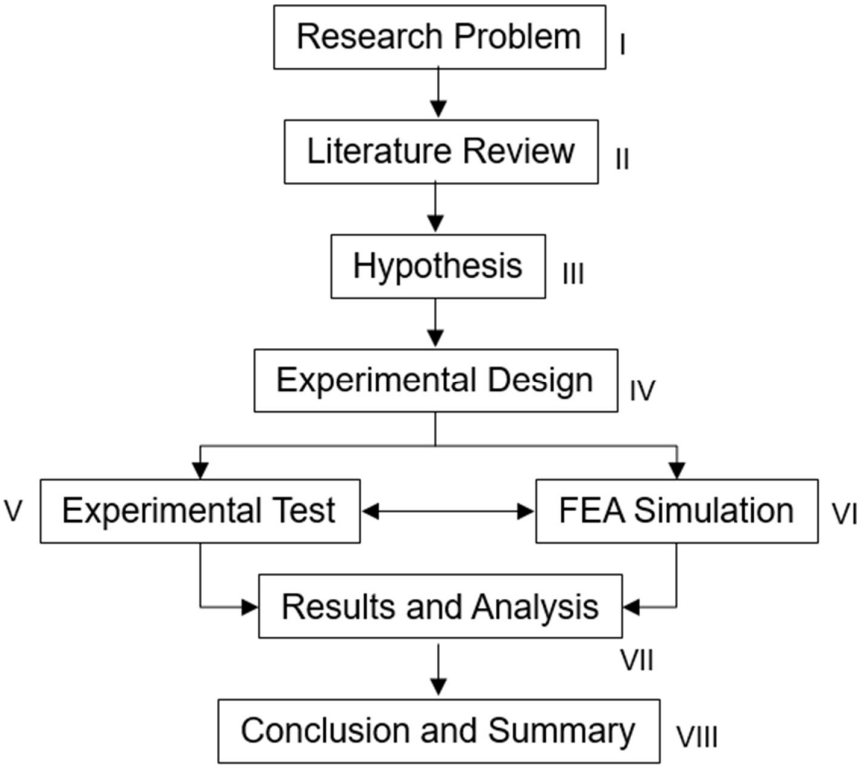

Figure 2. Flowchart of the research methodology.

In the fourth step, the experimental design has the role to define which welding parameters would be modelled and simulated. In the experimental tests, the results of experimental tests already accomplished are included in this step. Following in parallel, the fifth step, related to the FEA simulation are accomplished, with the input from the experimental tests, will be generated data that will be analyzed and compared with results already existent on the

literature review. In the next step, the results will be obtained, discussed and analyzed. At last, in conclusion and summary the results and all the steps of the research will be discussed, and a conclusion will be presented.

1.8 Delimitations and scope

The researcher delimited to investigate the influence of the heat in the AHSS/UHSS materials by the different welding parameters, besides the effects of the heat input in the microstructure formation of the UHSS. The findings of the present research are focusing on the AHSS/UHSS materials, particularly the 960 MPa grade that will be further evaluated.

In addition, the study limited to the GMAW process, since it is one of the process widely used along the designated material. The welding parameters selected to be evaluated are the current, voltage and welding speed, mainly due to have the greatest influence in the heat input of the already mentioned GMAW process. A single and multi-pass welding (with three passes) were also considered in the present research, since it also affects the temperature and consequently the microstructure on the welding zone. In this way, even though it has a significant effect on the heat input, other variables such as shielding gas, flow rate, welding position, thickness material, filler material and joint remains the same for all the specimens tested.

In the computational analysis based on finite element to simulate the effect of the heat on the welding, it was inserted the same geometry and material characteristics to all the tests, and the number of elements and nodes during the creation of the mesh, was also the same. The necessity to limit the variables are also a feature to better control the results and focusing only on the variables related to the hypothesis considered in the initial phase of the study. The number of tests used was considered enough to provide a generalized foundation to subsequent studies related to the UHSS that may be developed in the future.

2 LITERATURE REVIEW

Currently, there are many different grades of AHSS available, and each grade has its own characteristics that needs to be considered during its utilization in welding process. In this way, this chapter will cover the different types and grades of AHSS, as the GMAW process and the main parameters that can influence in the welding of AHSS. Additionally, the modelling and simulation methods used in the welding process will also be detailed.

2.1 Ultra-high strength steels

The steels are one of the major materials used in engineering during the building of structures and transports vehicles, such as cars. The reasons to the leading of steels throughout so many years are mostly related to its performance, manufacturability, recyclability, affordability and the possibility to be appropriate to many applications. Along the years and due to the high development of the technology, steels were developed, and the high-strength steels came as an evolution of the mild steels. If compared to other steels, the AHSS may not be considered lighter, but, due its high strength may provide thinner steel sheets or structures, reducing the weight of vehicles and decreasing the amount of material in a determined structure. (Demeri 2013, p. 1.)

In this way, it is also important to understand the role of AHSS if compared to other materials, such as magnesium, aluminum and some specific composites (for example the carbon fiber reinforced polymer) that also could offer the benefits of weight reduction. Although they are examples of low-density materials, their use in vehicles or structures does not necessarily mean a reduction of GHG. If compared to steels, the production of the low-density materials may produce 7 to 20 times more emissions (figure 3), what does not make these materials as eco-friendly as the steels if compared to the GHG emission. Another impact of those alternative materials is related to the cost, where they are more expensive and the utilization in low cost vehicles is still limited. (World Auto Steel 2017, p. 1-7.)

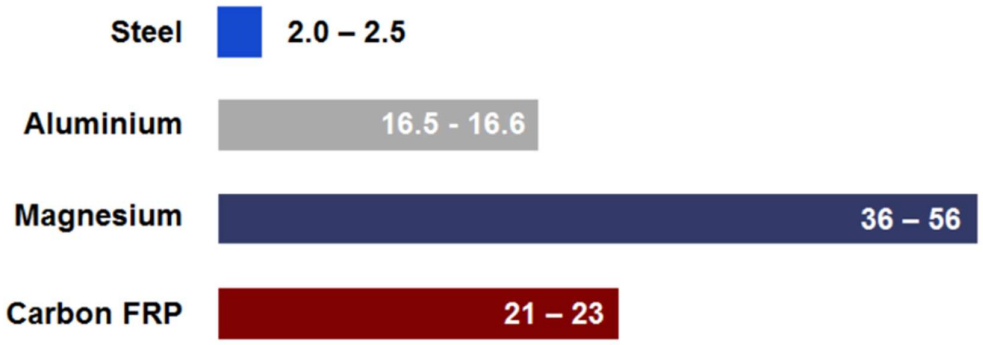

Figure 3. GHG emissions by material, in kg CO_2e/kg material (World Auto Steel, 2017, p. 1-7).

Initially, it is essential to define some terms used during the current thesis. The designations of AHSS and UHSS are terms that may vary along the present research depending of the author or source. Thus, to the steel manufacturing ArcelorMittal, the AHSS are the steels which the ultimate tensile strength (UTS) is between 450 and 800 MPa and the UHSS are those steels which the UTS is further than 980 MPa. However, there is also some sources that considers the UHSS with a UTS above 550 MPa and the AHSS as a major class where the UHSS is inside. Other sources consider that the term AHSS is designated to steels which the yield strength (YS) is above to 280/300 MPa and the tensile strength is above to 590/600 MPa with an enhanced formability. The definitions may be further if it relates to the process utilized throughout the manufacturing of the steel, which is suggested by some steel manufacturers. However, the definitions based in the ultimate tensile strength is still the most known and used. (McCallion 2012; Fonstein 2015, p. 5.) The present thesis will consider the designation of UHSS from all the steels that has an ultimate tensile and yield strength above 700 MPa and the AHSS mentioned will be relating the materials that has this same limit of ultimate tensile and yield strength.

A significant feature of AHSS is the several phases that offers increased properties such as strength and ductility that are not possible to reach along some single-phase steels as HSLA where the strength is achieved by alloying and solid solution hardening. In addition, a few alloying elements provided by a specific thermomechanical process aids to influence those characteristics. (World Auto Steel 2017, p. 1-3.) The AHSS are still in development, which may provide news designations and properties to the material. Parameters as strength and formability are being requested during the design of products that needs to offer a high level

of complexity that the thickness is reduced, and the stiffness needs to be guaranteed. The technology involved in AHSS support the possibility to optimize some technologies comprises by welding process, for example. However, due to the complexity and the many combinations of grades, applications and other issues, it is crucial that engineers with different expertise and commercial professionals work together in an integrated method. (Fonstein 2015, p. 5; Mohrbacher, Spöttl & Paegle 2015, p. 17.)

2.1.1 State of the art of ultra-high strength steels

The AHSS has been developed since early 1980s, starting the so-called first generation of this material. The first-generation of steels produced was based on ferrite and martensite microstructure, however, the tensile strength (between 700 to 800 MPa), the fracture toughness and the reducing of weight still did not reach the expected results. (3rd-generation advanced high-strength steel 2013, p. 10.)

The second generation of AHSS was developed around ten years later, aiming to improve the strength and fracture toughness along the reduction of weight. In this way, an elevated amount (20%-25%) of manganese was used to create a stabilized metastable austenite phase. It aided to enhance the strength and toughness of the steels based in the transformation of austenite phase in martensitic structure. In addition, the formability was improved since the first generation due the high austenite stabilizer. However, in the time that the strength was improved (800 to 900 MPa), the fracture toughness and the weight reduction still did not achieve required results. In addition, the cost it was very elevated due the high amount of manganese and nickel and the effort to process the steel due the high amount of austenite. (3rd-generation advanced high-strength steel 2013, p. 10-11; Demeri 2013, p. 18.) As can be noticed from figure 4, the relation between elongation and tensile strength presents the evolution and which part they are comprised by the first and second generation of AHSS. Besides, the conventional high strength steels (HSS) are showed to be possible to analyze the improvements related to the formability accomplished to this point by the AHSS.

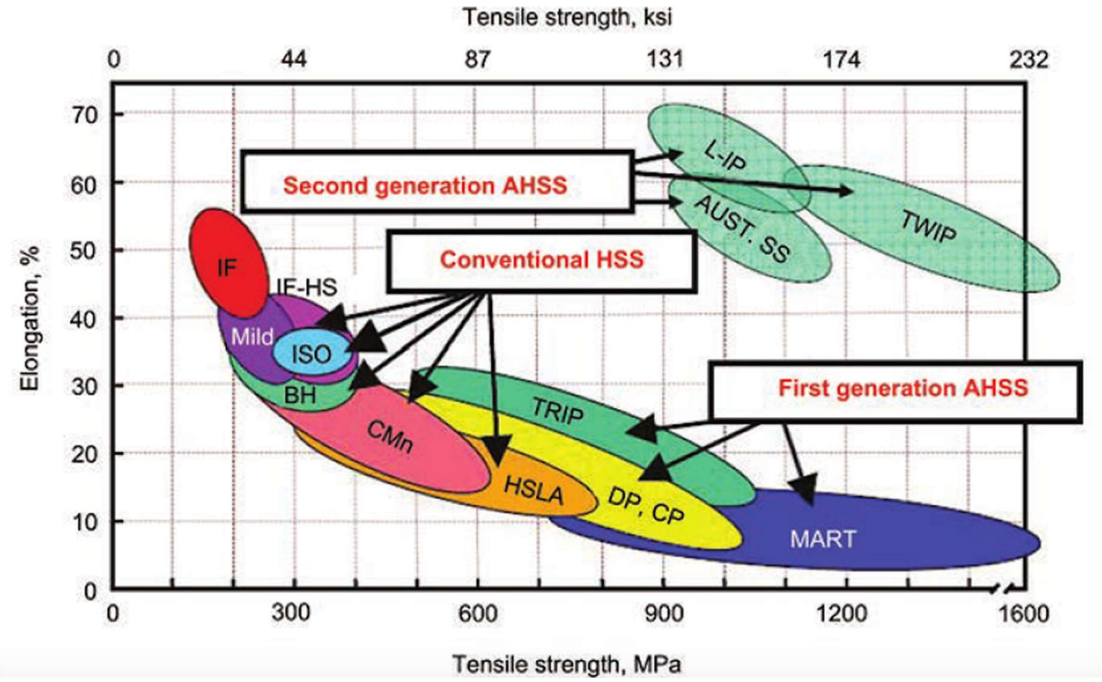

Figure 4. Relation between elongation versus tensile strength of the conventional HSS, first generation and second generation of AHSS (Demeri 2013, p. 18).

The advances achieved by the first and second generation of AHSS was undeniable, however, there was still the necessity to reach better results associated to higher strength and fracture toughness with a well cost-efficient production. In this way, according to Demeri (2013, p. 264), in 2007 a third generation of AHSS was developed to cover the necessities left by the previous generations wherein four requirements were considered as elementary requisites:

- High quantity of stable austenite;
- Low carbon content to ensure a good weldability;
- Low alloys content to decrease the cost;
- Production process compatible with the sheet steel process already existent.

Therefore, in the third generation of AHSS a high tensile strength and fracture toughness was achieved based in ultrafine grain ferrite and austenite, providing a dual phase microstructure. To obtain the desired results, the steel was also submitted by heat treatments as annealing and austempering, producing a bainitic microstructure with the austenite and a ferrite duplex microstructure. Besides, alloys elements were added to perform different roles during the fabrication process, either to improve or preserve some properties of the steel

during the austempering process (chromium, manganese and molybdenum) or even to prevent the creation of undesirable properties (as example the silicon that was used to inhibit the creation of cementite). As result, the tensile strength and the fracture toughness were significantly improved in the third generation of AHSS, obtaining the respective values of 1388 MPa and 105 MPa. Though the excellent improvements obtained from tensile strength and fracture toughness, the AHSS are still in development, aiming properties as the ductility that also aid the reduction of weight in vehicles or structures. (3rd-generation advanced high-strength steel 2013, p. 11.)

Figure 5 presents the results of the improvements achieved related to the global formability since the conventional strength steels until the third generation of AHSS, which may also reflect the wide range of mechanical properties of AHSS. According to McCallion (2012), the AHSS currently comprises a wide range of grades and types, since the dual phase until martensitic steels. Additionally, the techniques and methods used to strengthen the steels may also vary since a solid-solution hardening until grain refinement, resulting in different microstructures.

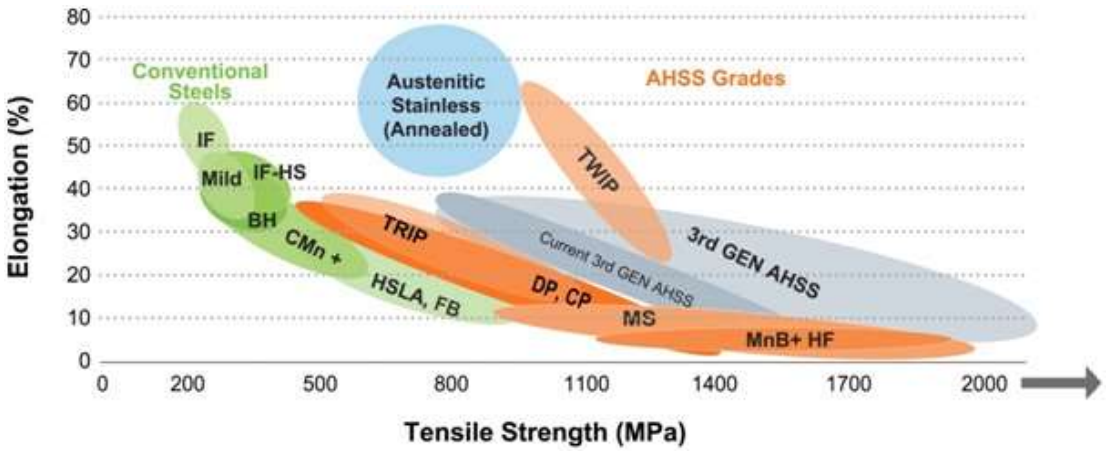

Figure 5. Relation between elongation versus tensile strength (formability) of the conventional steels, AHSS grades and the third generation of AHSS (World Auto Steel 2017, p. 2-1).

2.1.2 Grades and types

The grades and types of AHSS/UHSS are based on advances made from the HSSs. Consequently, the main difference between both types consists in their microstructure. Thus,

while HSS has a single-phase (ferritic) with the possibility to obtain a pearlite in some C-Mn based steels, the AHSS may contain a variety of phases such as ferrite, bainite, martensite, austenite and even retained austenite, which generate the complex and unique microstructure characteristic of the AHSSs. Besides the exclusive mechanical properties of AHSS, the equilibrium between strength and ductility is higher if compared to the conventional steels (HSS). To obtain the necessary knowledge about AHSS in its several applications, it is important to understand the behavior of the steels, like the phases, strengths, microstructures and thermal treatment process. (Demeri 2013, pp. 19-20; World Auto Steel 2017, p. 2-1.) Due to some different frontlines in the development of AHSS, some types and grades will vary depending of the author. In this way, Van Rensselar (2011, p. 42) shows in the table 1 the common steels types, since the standard steels until the advanced ultra-high strength steels (A-UHSS).

Table 1. Common steels types (Mod. Van Rensselar 2011, p. 43).

Common Steels Types		
Standard (Mild) Steels	**High-Strength Steels**	**Advanced Ultra High-Strength Steels**
- Commercial steel (CS) - Drawing steel (DS) - Deep drawing steel (DDS) - Interstitial-free (IF)	- Bake hardenable (BH) - Isotropic (IS) - Carbon-Manganese (C-Mn) - High-strength low alloy (HSLA) - Dual Phase (DP) - Complex phase (CP) - Transformation induced plasticity (TRIP) - Martensitic (MART)	- Dual Phase (DP) - Transformation induced plasticity (TRIP) - High hole expansion (HHE) / Stretch Flanging High-strength (SFHS) - Complex phase (CP) - Martensitic - Mn-B steel

The AHSS is also divided in different generations and contain grades with the goal to meet some specific requirements. According to World Auto Steel (2017, p. 1-2.), dual-phase and transformation-induced plasticity (TRIP) are examples of grades that has superior performance result to the absorb impact energy. However, if the intention is to protect the passenger and create a safety cell in a car, grades that are based on martensitic and boron-based press hardened steels (PHS) is a better option. Besides those mentioned grades, others such as complex-phase (CP), hot-formed (HF), twinning-induced plasticity (TWIP), ferritic-bainitic (FB) and martensitic (MS or MART) is also included in the AHSS family. (World Auto Steel 2017, p. 1-2.)

As stated by Van Rensselar (2011, pp. 40, 42-44), a mode to create the yield strength levels of steels is to base in the A-UHSSs grades. The author also mentioned five basic types of A-USS, which are: dual-phase, transformation-induced plasticity, high hole expansion (HHE)/stretch flanging high-strength (SFHS), complex-phase and martensitic. As a comparison, Demeri (2013, p. 264) presents on table 2 different grades and generations of AHSS along with other grades of material. The grades presented by both authors are basically the same, however, it is essential to understand that still there are some grades under development.

Table 2. Microstructural classes of conventional high-strength steels and three generation of advanced high-strength steels (Mod. Demeri 2013, p. 264).

Steel Grade	Microstructure
HSS	Ferrite-based
- Bake-hardenable (BH) - High-strength, low-alloy (HSLA)	
First-generation AHSS	Ferrite-based
- Dual-phase (DP) - Complex-phase (CP) - Bainitic - Transformation-induced plasticity (TRIP) - Martensitic (MS)	
Second-generation AHSS	Austenite-based
- Austenitic stainless (AUST SS) - Twinning-induced plasticity (TWIP) - Lightweight-induced plasticity (L-IP) - Others	
Third-generation AHSS	Multiphase: composite (austenite and martensite), ultra-fine-grained ferrite, martensite, stabilized austenite
- Under development	

As mentioned before, dual-phase is a material developed in the first generation of the AHSS and its main characteristic is the microstructure based on soft ferrite and hard martensite. Regarding to the strength level of dual-phase material, it is proportional to the quantity of martensite in the microstructure (figure 6 presents the dual phase microstructure). This characteristic provides to the dual-phase material improvements in some properties if compared to the HSLA, such as: formability, high strength and energy absorption. However,

regarding to the weldability, HSLA and DP has same grade. DP are commonly used in automotive industries, specifically on wheels and bumper reinforcement that requires high strength and formability (Van Rensselar 2011, pp. 40, 42-44.)

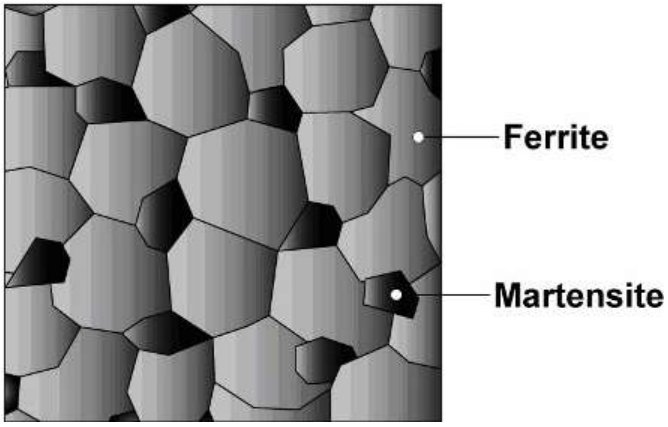

Figure 6. Schematic microstructure of DP steels (Mod. World Auto Steel 2014, p. 2-2).

The main difference between transformation-induced plasticity and dual-phase steels is the additional compound of bainite and retained austenite beyond existing soft ferrite and martensite on DP steels (figure 7 shows the microstructure of TRIP steels). However, while the TRIP benefits of the work-hardening on DP provide a better crash energy absorption, in compared to other AHSS in the same grade, the spot welding are still a challenge. (Van Rensselar 2011, pp. 42-44.)

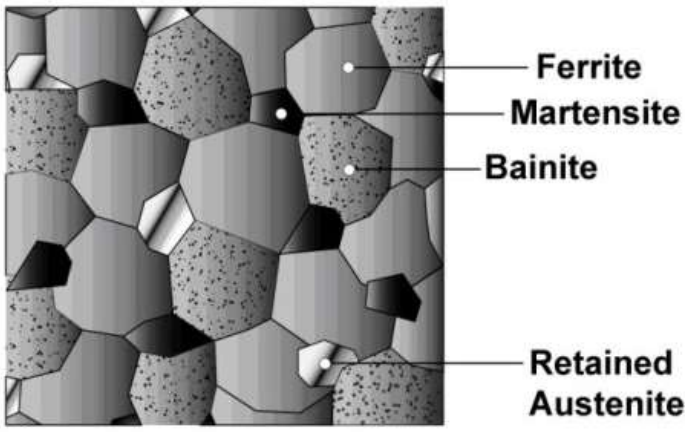

Figure 7. Schematic microstructure of TRIP steels, showing the ferrite, martensite, bainite and the retained austenite (Mod. World Auto Steels, 2014, p. 2-5).

The high hole expansion/stretch flanging high-strength steels are indicated to stamped parts due to its property of edge elongation. The expansion characteristic along high strength and high formability is given by a ferrite-bainite and a small quantity of retained austenite in its microstructure. Another AHSS steel grade also used on automotive industry, the complex-phase has significant results related to its properties of high energy absorption. Excluding the retained austenite, CP is like TRIP steels and may also reach a strength range from 800 to 1.000 MPa (145 KSI), which is accomplished by the microstructure composed from martensite and bainite phases along precipitations based on materials such as niobium, titanium or vanadium. (Van Rensselar 2011, pp. 42-44.)

As labeled by the name, the martensitic steels have a microstructure compound entirely by martensite. In this way, while the tensile strength tends to be high (between 900 and 1500 MPa) the elongation of the material is limited, which also directs the roll-formed process at a mill. Figure 8 shows the microstructure of a MS950/1200. (Van Rensselar 2011, pp. 40, 42-44.)

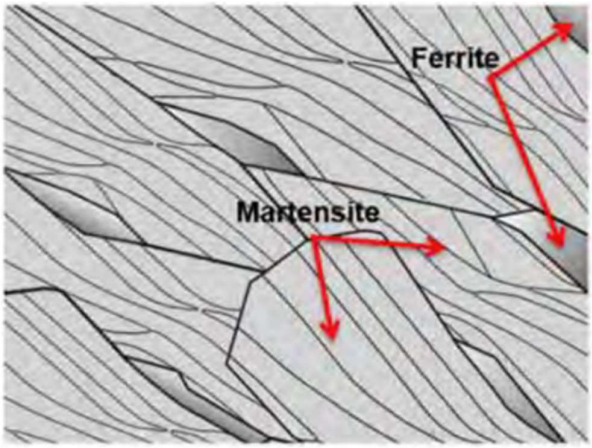

Figure 8. Schematic microstructure of a 950/1200 martensitic steels microstructure (World Auto Steel 2017, p. 2-10).

In addition to the martensitic steels, this material usually has a low content of carbon that along some chemical elements like Mn, B and Cr tends to improve the hardenability. Examples of applications to this material are those that involve high strength and fatigue resistance, such as side sill reinforcements and door beams of vehicles. (Van Rensselar 2011, pp. 40, 42-44.)

2.1.3 Applications of ultra-high strength steels

The selection of the materials that will be inserted in a determined product is directly related to the specific requirements and working environments. The UHSS is known as a structural steel, which favors its application in several different ways due to its ultra-high strength characteristic. In this way, according to a study of Guo et al. (2015, p. 534) related to the S960 UHSS, it was mentioned the employment of S960 in heavy crane industries, mainly due to properties as weldability, high strength, toughness and low weight. In addition, this material is also related to applications as oil and gas transportation pipes, offshore industries and shipbuilding.

In parallel, Demeri (2013, p. 9) mentions the utilization of AHSS in vehicles and the enhancement of fuel economy with the properly application of this material. Thus, if the AHSS is considered in a project of a car or light truck, it is possible to obtain a fuel economy of 6 to 8% for each 10% of weight reduced. Demeri also mentions the three approaches to reduce weight in vehicles:

1. Vehicle downsizing;
2. Modifications in the vehicle project;
3. Use of lighter/stronger material.

Thus, the option of downsizing is applied in some vehicles, but it is mostly restricted to a few components to avoid the reduction of comfort due to the preferences of larger vehicles costumers. The possibility to modify the project of the vehicle may produce minimum reduction in the weight. In this way, the option related to the utilization of lighter/stronger material appears as the most suitable. Therefore, the reduction of weight may be accomplished by substituting heavy components in specific regions of a vehicle as the body and chassis, which their sum corresponds to approximately 65% of the total weight of a vehicle. (Demeri 2013, p. 9.)

The application of AHSS is directly related and has a great benefit in materials where the strength prevails. In this way, if the work requirement of a component is relevant, a certain amount of deformation by load or even a determined amount of energy absorption is required, making the strength essential to support the expected results. It is also important to notice that the geometry along the yield and tensile strengths have a huge impact in the

strength of a project. A safety cell is an example where different load are applied and a desirable requirement is a minimum or even no deformation when a high strength is applied. To be able to reach this requirement, there are longitudinal and lateral beams with an inner and outer structure that coordinate the applied load, in a way to absorb the maximum energy. (Shome & Tumuluru 2015, pp. 10-11.) The figure 9 shows a safety cell of a car, where the advantages of the beams (longitudinal and lateral) structure were designed along with UHHS, improving the safety of the passengers and the driver.

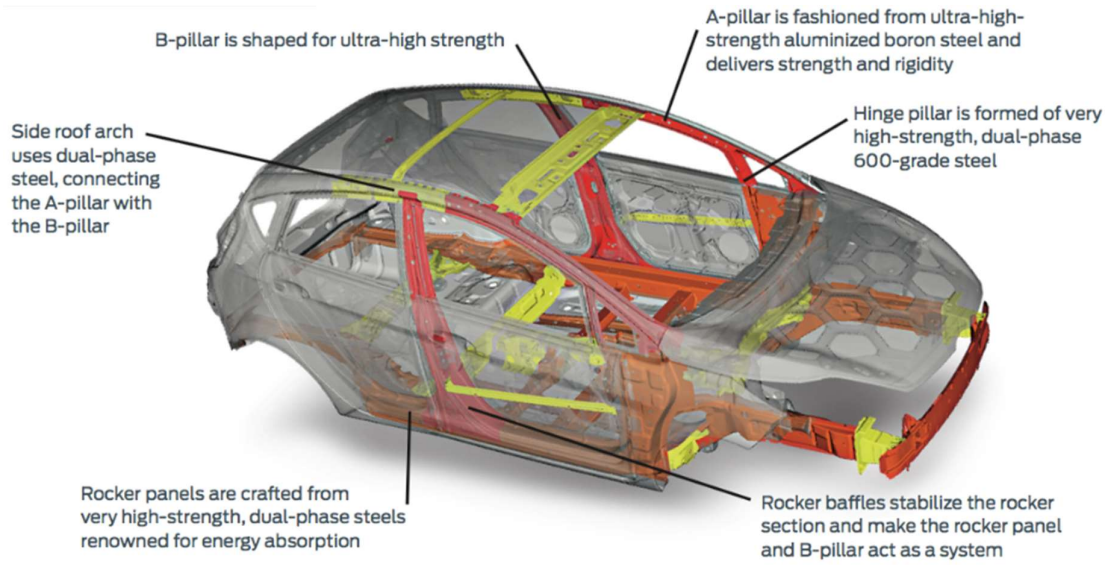

Figure 9. UHHS applied in a body in white structure of a European Ford Fiesta (Ford Motor Company 2011).

The steels used in truck cabins was mainly based in press stamped steel sheet. The mild steel (approximately 270 MPa tensile strength) was the most common material used, however, in the last 15 years, steels with higher strength was incorporate to the manufacturing of the cabins, allowed a small reduction of weight. In addition, dual-phase steels (500-650 MPa tensile strength) were used to absorb crash energy due its efficiency. (Mohrbacher, Spöttl & Paegle 2015, p. 5.) The enhanced crashworthiness of the ultra-high strength steels could also be noticed by Demeri (2013, p. 20), which mentioned the benefits to reduce the thickness of the material and keep the performance. Besides, along with the thickness reduction, factors as reduced of the material cost, increase in the fuel efficiency and benefits in environmental issues was also considered.

2.1.4 Issues on UHSS

The development of UHSS and its applications brought different perspectives to the conventional methods of production, mostly due the unique characteristics in the product/structures which UHSS is applied. These characteristics may bring not only advantages but also difficulties that needs to be discussed in the time that new materials are inserted in a way to prevent future barriers (Laitinen, Valkonen & Kömi 2013, p. 283). As advantage, one of the most important issues nowadays and probably in the future is related to the sustainability, and some features are mentioned by Demeri (2013, p. 257) that may bring benefits to this subject:

- Reduction of the steel used in products/structures due the high strength and the decrease of the material thickness;
- Reduction of pollution due the diminution of use of steel already mentioned and the decrease of vehicles emission by the reduction its weight;
- Material process optimization related to the energy utilized;
- The AHSS is a recyclable material;
- Increase of lifetime of the products due its enhanced performance.

Another approach brought from UHSS or very high strength steels (VHSS) as nominated by Qiang et al. (2016, p.60) is related to the benefits on logistics and operations. Thus, since to building a structure takes time and certain amount of material, by using materials that has a higher strength would decrease the transportation and reduces others process, such as the volume of welding used. Furthermore, the cranes and vehicles companies may also be benefited by the payload increase. Again, the environment issues regarding to saving energy is also mentioned as a huge benefit if compared to other materials.

On the other hand, the recyclability and the ways how the scrap of AHSS are handled needs to be analyzed in detail. Due the high alloys elements present in AHSS, utilizing the conventional recycle process may provide undesirable alloys. The recyclable process of AHSS can be considered more difficult to provide a high level of purity as a raw material. However, some steel manufacturers are developing new process to be possible its recycling and it may not be considered as a great difficult in a near future. (Alriksson & Henningsson 2015, p. 652; Demeri 2013, p. 260.)

The high strength levels reached by the newest generations of AHSS also has some difficulties related to the safety. An important issue of the high strength is associated to the necessity to accomplish an emergency rescue in a vehicle that the AHSS is applied. In a car crash situation, if the vehicle is composed by AHSS material, the rescue tool available to tear the sheets may not be enough or even not work during a rescue. The knowledge of the rescuers related to the materials inserted in a vehicle are limited and in a scenario of urgency as a car crash, the time and the properly work of the rescuer's tools are essential to save life. (Van Rensselar 2011, pp. 43-44.)

According to a study accomplished by Alrkisson & Henningsson (2015, pp. 653-654), it was described the main barriers throughout introducing of new materials, which in general is a process that takes time. In this study, the AHSS was analyzed and the main conclusions obtained were related to some factors as the necessity of knowledge of the material not only in the manufacturing process itself, but also by the whole supply chain. In addition, an essential issue that may facilitate the process of a new material introduction is related to the communication between all the interested parts. In this way, essential information as: costs, environmental issues, design and manufacturability are very important to avoid eventual barriers during the implemental of a new material as AHSS.

2.2 GMAW in Ultra-high strength steels

The welding process involved in AHSS is critical and requires a necessary control and knowledge during its execution. The GMAW has a great flexibility and is broadly used for several applications, which became very useful to welding AHSS, since it is an established welding process. Since the GMAW process operates with a continuous filler metal shielded by an external supplied gas along an automatic feeding (see the GMAW operation in figure 10), another advantage is related to the automation using robots. In this way, due to the self-regulation of the arc voltage and the wire feed speed, the travel speed and the course of the torch is the only needed to be led. While the most known commercially materials and all the position can be welded by GMAW, the better results may be achieved by the properly adjustments of the welding process variables. (O'Brien 2004, pp. 117; 148-150.)

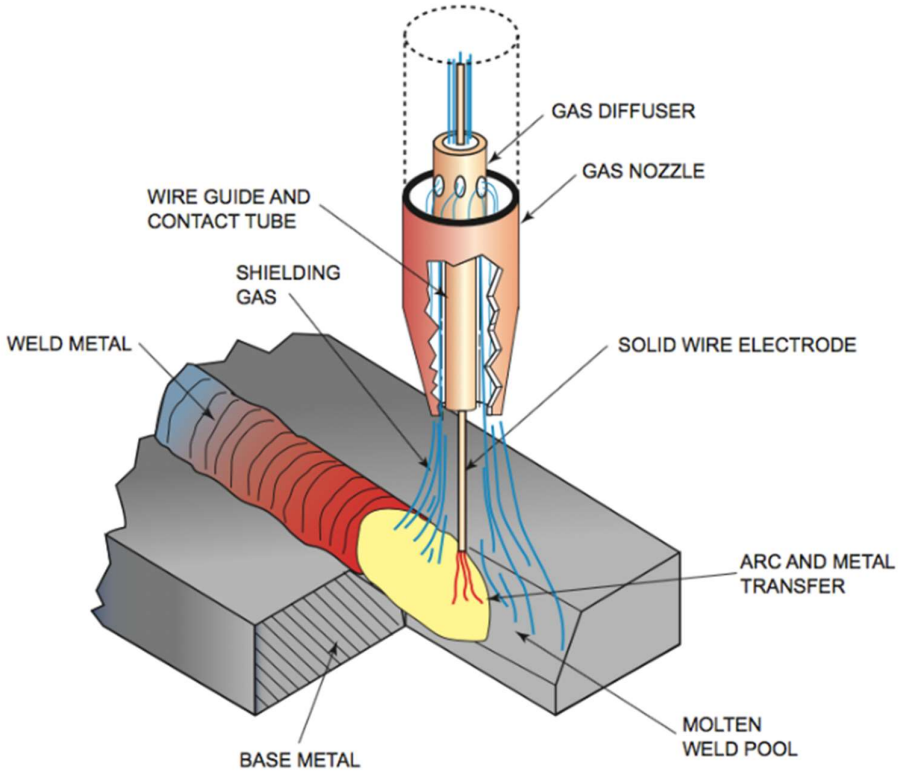

Figure 10. Gas metal arc welding operation (Jeffus 2012, p. 235).

In addition, a research related to UHSS accomplished by Mohrbacher, Spöttl & Paegle (2015, p. 7) mentioned that by using the GMAW process, the microstructure in the heat-affected zone (HAZ) and consequently the strength and impact toughness are directly influenced by the changes on the chemical composition (filler metal) and heat input applied on the steel during the welding. In this way, it is essential to have knowledge and experience to control the main variables in the welding process and then optimize the process to obtain suitable results. Base material, electrode composition and welding position are examples of parameters that may be changed and perform different results with many set possibilities. (O'Brien 2004, p. 117.)

2.2.1 Weldability

In the search of satisfactory quality in a way to assure the desired properties on the welding, the weldability must be considered, especially when an UHSS material is being welded. To exemplify, a 900 MPa yield strength steel grade generally has a worse weldability than a 700 MPa yield strength with the same type of steel. This occurs due to a microstructure characteristic of a material that has a higher yield strength based on a higher carbon

equivalent and increased hardenability, specifically, a sensitive microstructure. (Mohrbacher, Spöttl & Paegle 2015, p. 9.)

A study carried by Martis, Putatunda & Boileau (2013, p. 168.) showed a difficulty during the welding in steels with high carbon content (around 0.4%) and consequently high carbon equivalent. In this way, a recommended carbon content should be below 0.1%, which is preferable to be prioritized if compared to a low carbon equivalent. The mentioned key value was obtained by studies that were accomplished in succeeding manufacturing processes where high strength steels grades were used on the production of vehicles. In this way, the weldability and formability were the evaluated processes variables. (Mohrbacher, Spöttl & Paegle 2015, p. 17.)

2.2.2 Metallurgy

The third generation of AHSS introduced the known elevated strength along a high fracture toughness, which is a resultant of processing and alloying. The microstructure is composed by at least two phases with an essential feature, where the austenite has a key role in the microstructure. Since the stable retained austenite has significant quantities, it aids to preserve the ductility of the AHSS. However, due to its equilibrium phase, it is still a challenge to control and stabilize this high quantity in the ultimate steel microstructure. (Demeri 2013, pp. 264-265; Martis, Putatunda & Boileau 2013, p. 174.)

In other study accomplished by Aydin et al. (2013, p. 507), it was mentioned that not only the retained austenite has to be taking into consideration regarding to the mechanical properties, but also the transformed martensite sizes. Thus, with a higher martensite content, the strength also raises and the ductility decreases. In addition, it is not only the retained austenite content that has an influence on the ductility, but also with the increase of Mn content. The figure 11 illustrate the thermal cycle of the steel and when each phase may be reached.

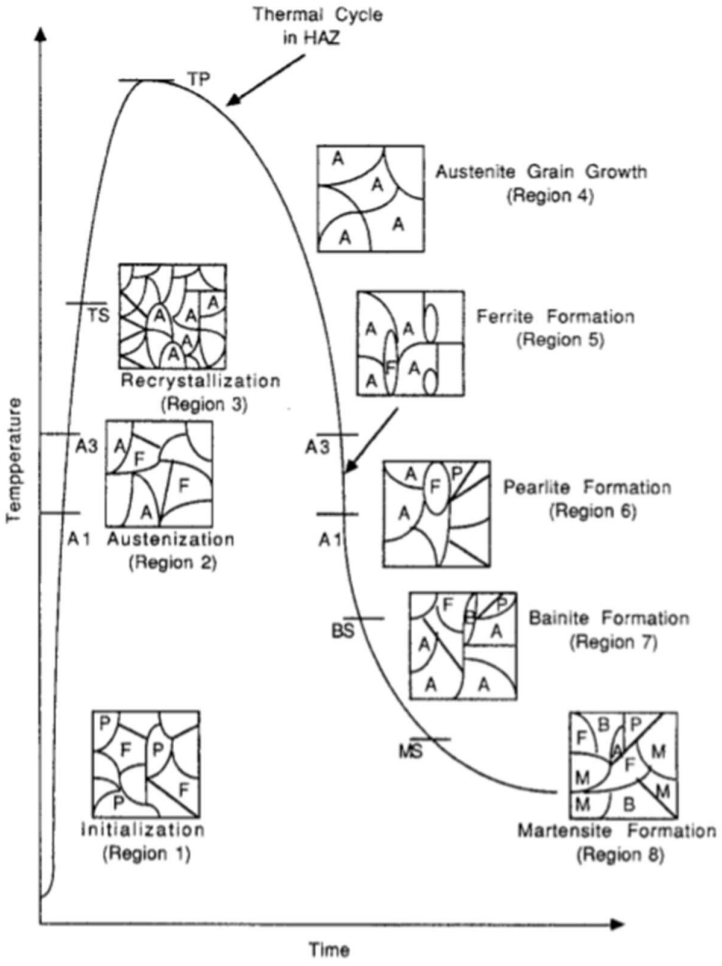

Figure 11. Transformations regions representation in a thermal cycle (Goldak & Akhlaghi 2005, p. 121).

Regarding to the chemical composition of the steel grades with higher strength, the low carbon content (range of 0.08% - 0.10%) along micro alloying elements as niobium (0.03%) and titanium are commonly used. These dual elements aid in the formation of polygonal ferritic and bainitic microstructure, with an extra credit to the niobium, that is used as a finest alloy to this type of steel grade. In addition, the pearlite is rather excluded due to its capacity to provide an undesirable decrease in the level of bendability (Mohrbacher, Spöttl & Paegle 2015, p. 8.)

Other micro alloying elements may be considered to obtain other properties; however, it also must be added to the several options of heat treatments that may lead to different property results. Thus, Van Rensselar (2011, p. 43-44) mentioned that the first alloying component

used to increase the strength of steel is the carbon. Though, it is essential to consider that the cost is also increased depending of the alloy amount and the metal involved. Another consideration remains in the process related to the AHSS that affects the crystalline structure by the temperature introduced. To be possible to obtain the necessary strength without to add a great amount of alloying, the steel sheet is rolled again (the first time was in the early process) in a room temperature and then a controlled high heat is imposed along a quick cooled process (that may be used annealing and quenching). Thus, the austenite is changed to martensite. This controlled and precise thermal process along the micro alloying elements are the responsible to provide the strength and formability characteristics of this steels grade, since the ferrite and martensite are well handled.

Demeri (2013, pp. 264-265) reinforces the critical stage that is accomplished during the manufacturing of the steels, since to obtain an optimized material, the control associated during the process is fundamental. The strength and ductility perform a key role in those steels, since it must to bear high loads and in the same time, allow the steels to form parts. Those properties are better achieved along the use of some heat treatments as quench and temper, which together to the restricted addition of alloying elements (again to reduce cost) compound the main objective of the third generation of AHSS.

Relating to the properties of the UHSS, Neimitz, Dzioba & Limnell (2012, p. 25) evidenced that the characteristics of a S960 QC steel is unusual if compared to the conventional ferritic steels. In this way, they accomplished a study to understand the behavior of the material that is not suitable to a typical material master curve. As an example of result, it was observed that there was no difference beetween the a range of 4 to 8 mm thickness plate regarding to fracture toughness.

2.2.3 Heat input

The heat input has a main role in the welding, since it affects directly the microstructure of the fusion area and the heat affected zone. This last one is comprised between the solid-liquid transition and the base metal (see figure 12). The effects of the thermal cycle during the welding process are the changes generated on the steel that can make the material harder and more vulnerable to brittle fracture (with large austenite grain size). Other properties

coming from the thermal cycle lead the material welded to be more sensitive to stress and corrosion, among other characteristics. (Goldak & Akhlaghi 2005, p. 119-120.)

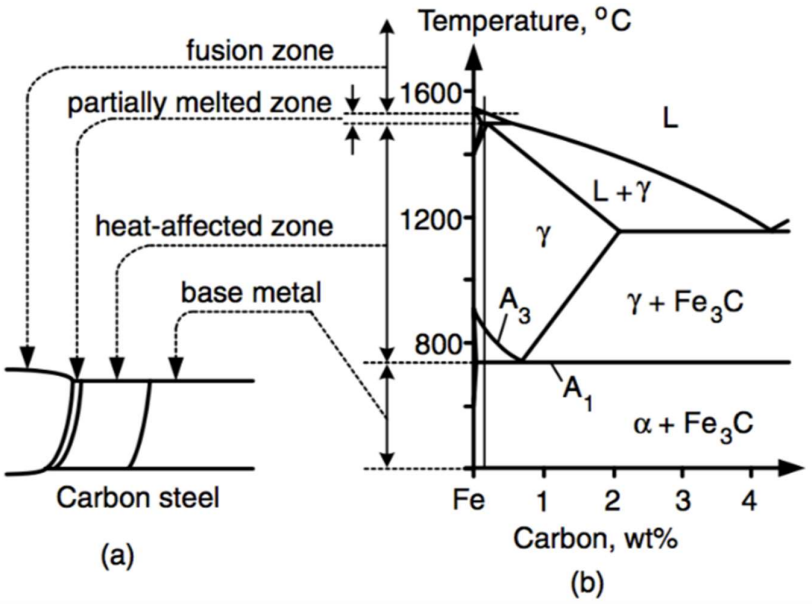

Figure 12. Welding carbon steel: (a) HAZ and (b) phase diagram (Kou 2003, p. 395).

In order to obtain the value of heat input, some welding parameters are considered. The heat input for arc welding may be calculated by the following equation:

$$Q\ (J/mm) = \frac{(E\ x\ I)\ x\ \eta}{v} \quad (1)$$

In equation 1, Q stands for heat input (J/mm), E is voltage, I is current, η is the arc efficiency and v is welding speed (mm/s) (Poorhaydari, K., Patchett, B. & Ivey, D. 2005, p. 151-s). The influence of the heat input should also be considered along the grade of welding wire used, since the chemical composition of the welding wire may affect the final result. In this way, Mohrbacher, Spöttl & Paegle (2015, p. 8) mentioned that to achieve better tensile strength results for a 700 MPa grade steel, the heat input must be restricted to a maximum of 11 kJ/cm (1.1 kJ/mm). Regarding to the welding wire, by using an overmatching wire (above the strength of the base material) it will head to the rupture in the weld metal, instead of the undermatching that heads to the rupture in the weld metal.

In another study carried out by Nowacki, Sajek & Matkowski (2016, pp. 783) with the aim to evaluate the influence of the welding heat input, it was demonstrated that the control of the heat input lead to a certain degree of refinement on the microstructure that may be adjusted according to the necessity. This study was accomplished on a UHSS material and compared 0.6 kJ/mm and 0.7 kJ/mm heat input.

2.3 Simulation and modelling in welding

The requirements of the current market enforce the necessity to use more efficient technologies to develop the products as CAx (computer-aided technologies) and FEA tools. Additionally, the possibility to use these tools allows to reduce the development time of a product and provides design techniques which the software used are in a full associative way, where the changes of a CAD (computer-aided design) file are made without data transfer to a CAE (computer-aided engineering) tool, for example. (Bozickovic et al. 2015, p. 165.)

However, most of the simulation softwares available nowadays perform different applications but only a few that are designed specifically to welding simulation. The multi task simulation softwares offers excellent results but the time spent used to modeling a specific welding operation needs to be optimized. (Perret et al. 2011, p. 896.) Thus, the necessity to obtain faster and cheaper results and consequently products with a high quality, stimulate the development of specialized and user-friendly simulation softwares in welding process.

The numerical calculation of heat flow in fusion welding generally requires a huge time to compute, mostly due to the high complexity (see an example of variables involved on the figure 13) to perform a reliable evaluation along an elevated cost. In the same time that these calculations have drawbacks, it also has a great potential to provide essential information regarding to the welding (geometry, composition, structure, among others) to predict and contribute with quantitative information to develop each time more those processes. In addition, the understanding of heat flow models has also to keep up the same pace of the tools used to perform the analysis. (Jenney & O'Brien 2001, p. 111.)

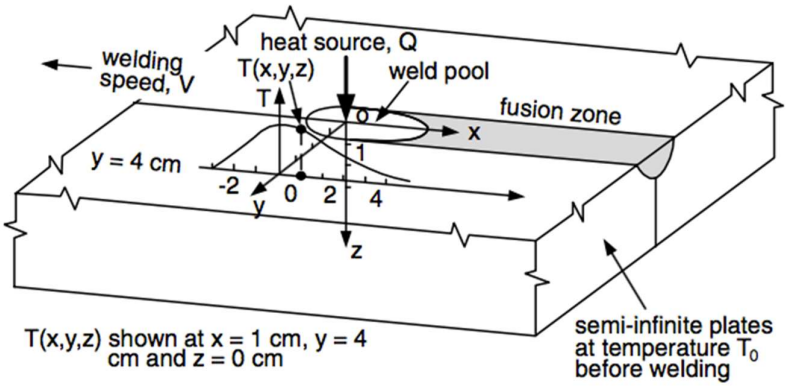

Figure 13. Rosenthal's three-dimensional model of welding heat flow (Kou 2003, p. 51).

An example of the applications in simulation of welding process is a study accomplished by Kravoskyy & Virta (2015, p. 2) related to the fatigue in welded joints. The study presented results which microstructure, residual stresses and the mechanical properties of a model could be simulated. The aim of the study was not only to evaluate the welded joints but also obtain beneficial results related to the cost. The simulation softwares needs to be selected according to the necessity of what will be evaluated, which in the welding process is mostly divided by the stages of the process, considering that the softwares are focused in some specifically purposes.

3 EXPERIMENTAL PROCEDURE

In the current chapter, the experimental design with a physical model along a simulation of the welding will be accomplished according to the figure 14. Thus, a physical model corresponds to an example of an application that will be performed in order to obtain results to be used as input to the subsequent steps.

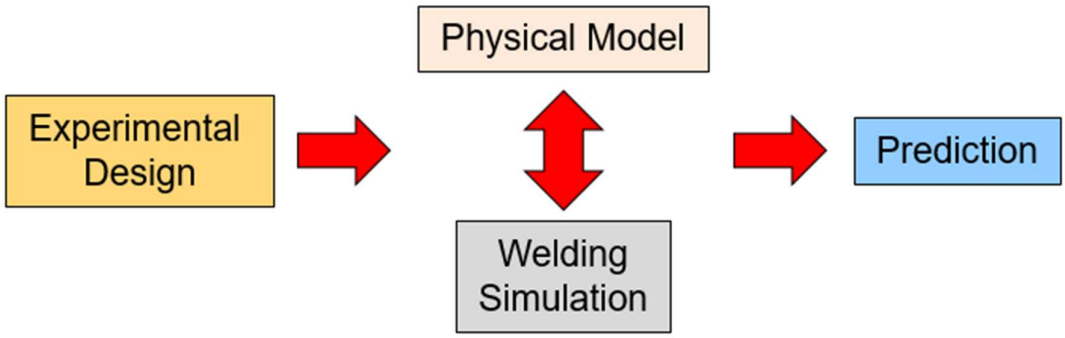

Figure 14. Flowchart of the experimental part.

In the physical model, some equations used in the experimental design to describe some behaviors will be analyzed. In addition, the welding simulation will replicate the physical model along with the results obtained during the experimental design. These two steps will be executed in parallel due to the possibility of update some values in the mathematical model stage and then perform the simulation (or vice versa) as an iteration way to reach a satisfactory result. The next and last step is the prediction itself, wherein the most important is to create a reliable prediction result, enabling to predict different welding conditions related to the physical model previously described.

3.1 Material properties

During the experimental tests, it was used a base material and a filler material to accomplish the welding. The base material was the UHSS Optim® 960 QC (quenched and cold formable), with 5 mm of thickness. The base material was provided by Ruukki company, followed by a material certificate (Appendix I) with the necessary information related to the metal.

In addition, to be possible to understand the metallurgy and weldability effects during the welding, it was essential to calculate the carbon equivalent (CE). The CE obtained in the present study was calculated based in the following equation recommended by International Institute of Welding (IIW):

$$CE = C + \frac{Mn}{6} + \frac{Cr+Mo+V}{5} + \frac{Ni+Cu}{15} \quad (2)$$

In equation 2 the *CE* is the carbon equivalent, *C* is carbon, *Mn* is manganese, *Cr* is chromium, *Mo* is molybdenum, *V* is vanadium, *Ni* is nickel and *Cu* is copper (O'Brien 2011, p. 43). Along with the chemical composition obtained by the material certificate of the base material, it was possible to calculate the CE of 0.47 (table 3). Based on the CE, the weldability of the S960 is good and no preheating was needed to accomplish the welding of a 5 mm thickness plate.

Table 3. Chemical composition and carbon equivalent of the base metal S960 steel (wt. %).

C	Si	Mn	P	S	Al	Cr	Mo
0.09	0.21	1.05	0.01	0.004	0.03	0.82	0.158
Ti	**B**	**Nb**	**Ni**	**V**	**Cu**	**Fe**	**CE**
0.032	0.0019	0.003	0.04	0.008	0.025	Balance	**0.47**

The mechanical properties of the UHSS 960 QC are shown in table 4. In the table is also presented information related to the specification and the measured values. In the case of the measured condition, the values presented were obtained by the information provided in the material certificate.

Table 4. Mechanical properties of the base metal UHSS S960 (Ruuki 2010).

Result	Yield strength $R_{p0.2}$ [MPa] Min.	Tensile strength R_m [MPa] Min.	Elongation [%] Min.	Impact work -40º C [KV J] Min.
Specification	960	1000	7	33
Measured	976	1108	12	74

The filler wire material used in this study was the Union X 96 (ER120S-G), a solid wire with a diameter of 1.0 mm. The chemical composition and the respective CE of the filler material

are shown in the table 5 and the table 6 presents the mechanical properties of the filler material.

Table 5. Chemical composition and carbon equivalent of the filler wire Union X 96 (wt. %) (Mod. Böhler Welding 2014).

C	Si	Mn	Cr	Mo	Ni	Fe	CE
0.12	0.80	1.90	0.45	0.55	2.35	Balance	**0.79**

Table 6. Mechanical properties of the filler wire Union X96 (Mod. Böhler Welding 2014).

Yield strength $R_{p0.2}$ [MPa]	Tensile strength R_m [MPa]	Elongation [%]	Impact work [KV J]	
			+20 ºC	-50 ºC
930	980	14	80	47

3.2 Welding setup

To accomplish the experimental tests, the base metal was fixed in a workbench through fixtures and it was linked to five thermocouple probes (figure 15). The utilization of the thermocouple's probes allowed to measure the temperature in the region of the welding during a certain time. In this way, it was possible to obtain values related to the peak temperature to auxiliary the understanding of the changes in the microstructure of the weld.

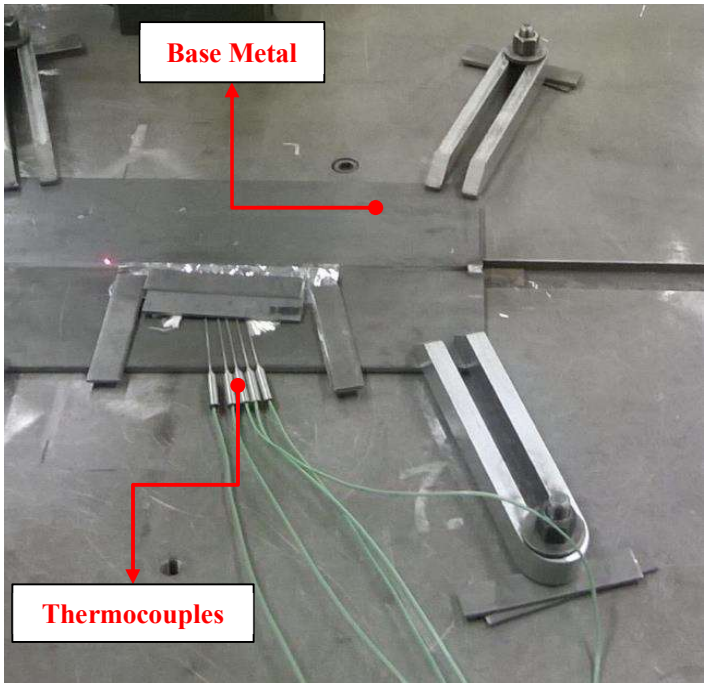

Figure 15. Thermocouples and base metal positioning.

The thermocouples probes were positioned in different coordinates of the base material, to be possible to evaluate the thermal cycles and the microstructure changes based on the temperature variation in different regions of the welding. The figure 16 shown the 5 drilled holes to positioning the thermocouples.

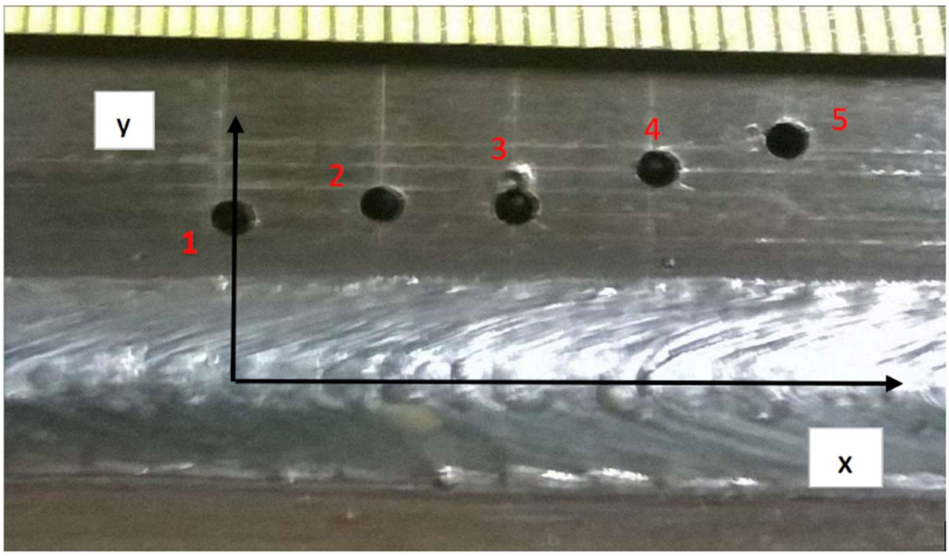

Figure 16. Location of the five (5) thermocouples probes in the experimental piece.

The coordinate position of each thermocouple probe may be seen in the table 7, showing in millimeters the location of each thermocouple probe. The positions are based on the axis X and Y showed in the figure 16.

Table 7. Positioning coordinate of the thermocouple probes (in millimeters).

Probe	X	Y
1	0	6.8
2	5	7.5
3	10	7.4
4	15	9.2
5	20	10.5

Another aspect during the welding setup is related to fixtures. The fixtures were used to hold the plates in the correct position and maintain the conformity along the welding process. In addition, it was used a welding robot (figure 17) to perform the welding. The welding robot

used in the present study is capable to welding by GMAW and its manufacturer is ABB Group.

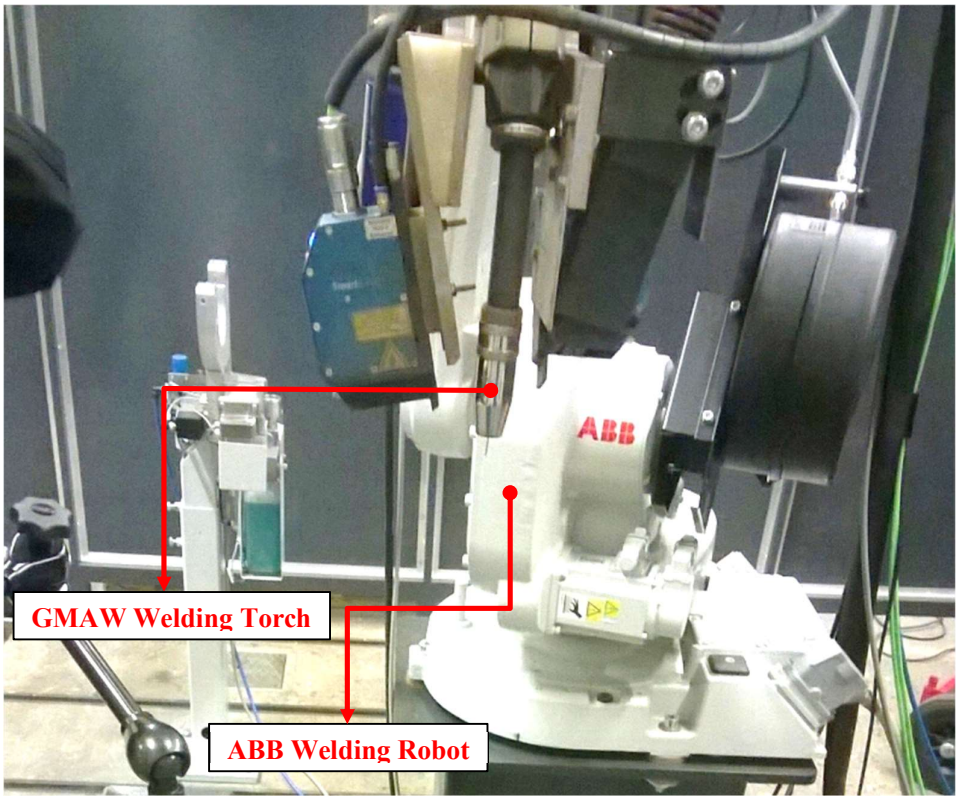

Figure 17. ABB welding robot utilized during the experiment.

In the figure 17 is also possible to visualize the manipulator of the robot settled with a torch of the GMAW process. The utilization of a robot allowed a more consistency during the welding, mainly due to the advantage to keep the same velocity and position, avoiding excessive variations along the process. The welding process performed by a robot will also reduce a variation in the penetration of the welding.

3.3 Weld joint and welding parameters

In the present study, the joint selected was the butt joint with a square groove weld type configuration. The choice of this type of joint was due to the lower thickness (5 mm) of the base metal. In this way, the welding parameters and conditions were defined based on the welding process and in the chosen joint. The shielding gas used to protect the welding was a mixture of 90% argon with 10% $C0_2$, with a flow rate of 16 l/min. The welding position

was the flat position (PA), with a stick out length of 18 mm and the wire feed rate was 9 m/min. Related to the air gap, it is important to mention that the gap varied along to the groove from 0 mm to 0.5 mm, mainly due to the deformations from the base material.

Other important parameters utilized during the experimental test are shown in the table 8. In the table are described the welding pass, voltage, current, welding speed, efficiency and heat input. Due to the thickness of 5 mm of the plate, it was necessary only one (1) welding pass. The efficiency of the GMAW process considered in this experiment was defined as 80%.

Table 8. Welding parameters used during the welding of the experimental test.

Welding pass	Voltage (V)	Current (A)	Welding speed (mm/s)	Efficiency (%)	Heat input (kJ/mm)
1	24	180	7	80	0.49

During the experimental test, the main parameters such as voltage, current and welding speed were defined based on the experience of the researchers of welding laboratory, however, in the next steps of the development of this study, different values of these variables will be considered. Additionally, during the welding of a sensitive material such as UHSSs, the heat input value is essential to understand the behavior of the material while a determined amount of heat is defined.

3.4 Welding simulation development

During the welding simulation, a virtual model was analyzed by finite element analysis to compare the results found in the experimental test with the physical model. To perform the FEA it was used the academic version of the software ANSYS R15.0. To reduce the computational processing time, the size of the specimen was purposely small. However, with satisfactory results acquired by the reduced size model, in further studies will be possible to simulate larger models.

In the experiment test with the physical model it was used only one-dimension thickness of the material. However, in the virtual model will be used the same 5 mm thickness used in the physical model along the single and multi-pass welding in the S960 UHSS material.

Therefore, to accomplish the welding simulation, it was also used the butt joint with a square groove configuration. The groove configuration was selected based on the thickness of the material, since the square groove was the same to the physical model, it will be used in the single and multi-pass welding. The groove weld utilized during the simulations and the dimensions of the virtual plate is detailed in the figure 18.

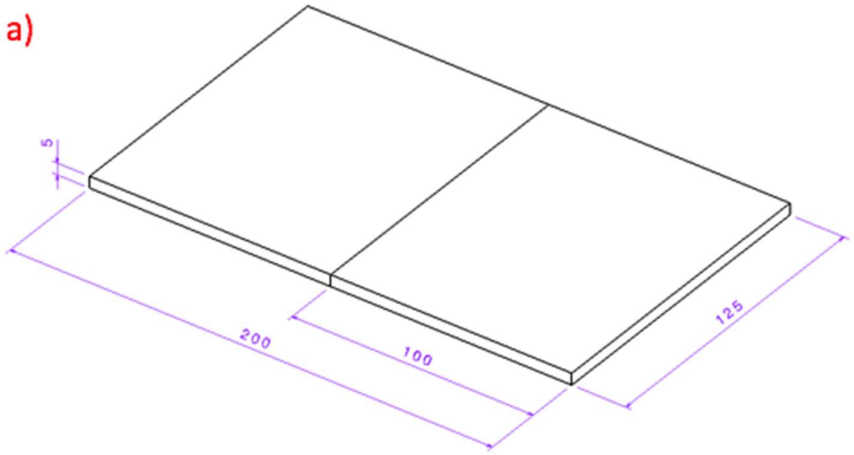

Figure 18. Geometric dimensions of the weld plate used in the welding simulation.

Throughout the figure 19 is also possible to see the differencies of the groove weld type and the thickness between the virtual specimen. The square groove may provide a full penetration in a 5 mm material. The figure 19 presents a front view with the dimensions of both groove weld used in the welding simulation.

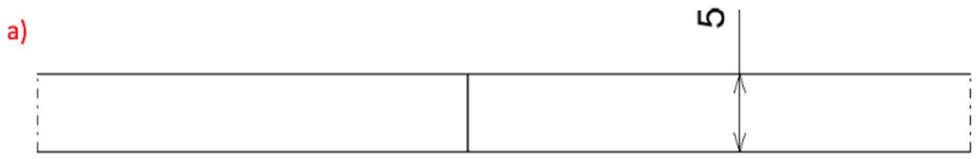

Figure 19. Geometric dimensions of the square groove weld used in the welding simulation.

Along with the geometric dimensions of the model, it was also necessary to generate a mesh in the virtual model. A mesh in a simulation by FEA is a technique to divide the whole model in small elements in order to make and ease the necessary calculation. In this way, a refined mesh was created along all the material. The total number of elements are 2.220 and the total

number of nodes are 16.216. The figure 20 shows the virtual model after the creation of the mesh.

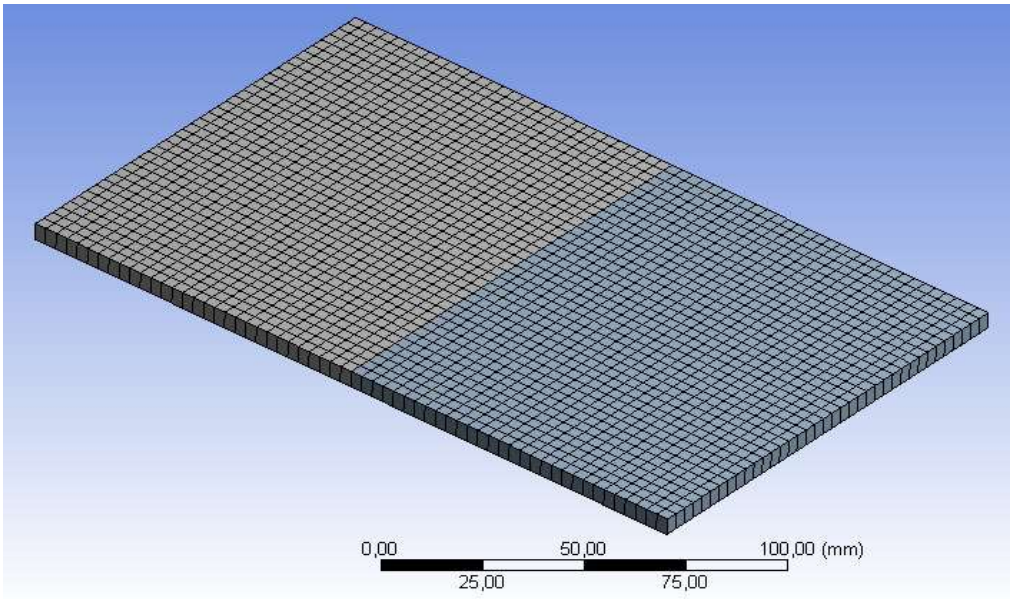

Figure 20. Mesh created on the finite element model.

In order to compare the results between the physical and the virtual model, five (5) thermocouples was inserted in the finite element model. The position of the probes has remained the same used of the physical model (figure 21). In this way, the use of thermocouples allowed to understand the amount of heat inputted by single and multi-pass welding.

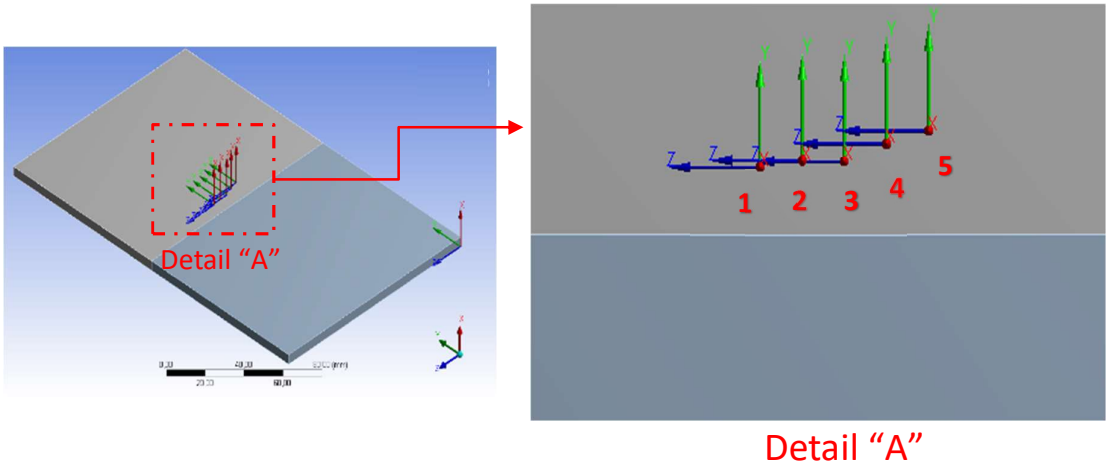

Figure 21. Location of the five (5) thermocouple probes in the finite element model.

In the welding simulation will be used two different amount of heat input in each welding pass. The table 9 shows the welding parameters used during the analysis, however, as the finite element analysis only consider the welding speed and the heat input, the other variables will be filled in a way to reach a desired amount of heat input to be analyzed.

Table 9. Welding parameters used during the welding simulation by finite element.

Welding pass	Voltage (V)	Current (A)	Welding speed (mm/s)	Efficiency (%)	Heat input (kJ/mm)
1	24	180	7	80	0.49
2	30	290	8.3	80	0.84

Therefore, it was selected two different ranges of heat input, since in the experiment of the physical model was used a 0.49 kJ/mm, in the virtual model will be also used an amount higher (0.84 kJ/mm) than the used in the physical model. In this way, the influence of heat will be better understood in a comparison way by the material of 5 mm thickness. The amount of the heat input of each simulation will be according to the above and already mentioned table 9.

Additionally, it is important to mention that the finite element analysis will be responsible to evaluate the thermo-mechanical behavior of the virtual models. Initially the simulation of the welding process will consider the transient thermal and after that will be considered the obtained information as an input to the thermal stress analysis. Thus, the present study will provide information related to the distortions and stresses, in a way to analyze the influence of the amount of heat input. In order to obtain the results, the ANSYS software is based on the Gaussian heat source wherein the moving heat flux is calculated from the following equation:

$$q = C_2 e^{\frac{[(x-x_0)^2+(y-y_0)^2+(z-z_0)^2]}{C_1^2}} \quad (3)$$

In equation 3, q is the heat flux, C_1 is the radius of the beam, C_2 is the source power intensity, x, x_o, y, y_o, z and z_o are the position of the center of the heat flux in a determined route, at the distance of the velocity (v) of the moving heat source multiplied by the time (t) from the start

point (ANSYS 2016, p. 9). The figure 22 presents the way how the heat flux in the equation 2 is obtained.

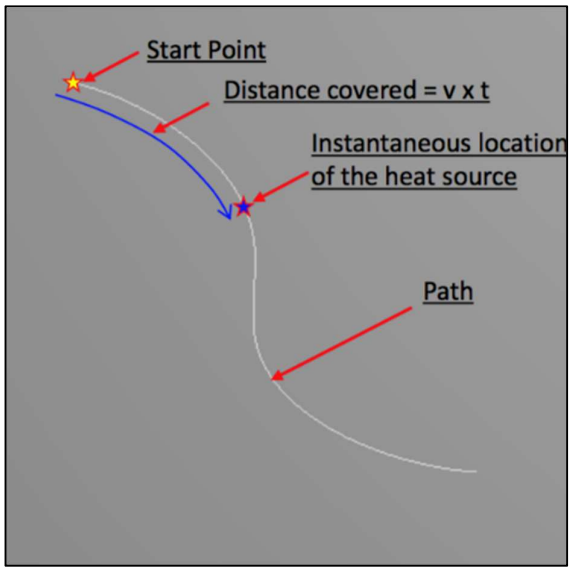

Figure 22. Description of the Gaussian heat flux source (ANSYS 2016, p. 9).

4 RESULTS AND ANALYSIS

In this chapter will be presented the results found during the experimental tests, which includes the physical and virtual experiment. In order to obtain a better understanding of the results and its effects, the analysis will be also accomplished in this chapter.

4.1 Experimental tests results

In order to be possible to optimize the GMAW process parameters, the influence of the heat input is essential to understand the effects of each parameter. Beside the increase of quality and reliability in a structure, the right choose of the welding parameters are also important to avoid the waste of unnecessary energy to accomplish a welding.

The experimental test was carried out in the welding laboratory of the Lappeenranta University of Technology. With the aim of complete an efficient experimental test, some essential variables were evaluated to better comprehend the performance of the GMAW process parameters along UHSS material. In this way, a macrostructure, microhardness and an evaluation of the thermal cycle were accomplished.

4.1.1 Macro etch cross section of the weld joint

The macro etch cross section on a weld joint may be accomplished to evaluate welding structures in order to visually obtain results related to the weld penetration, dilution, dimensions and other general characteristics that may be evidenced only by using the macrostructure. In this manner, a macro etch cross section was accomplished on the physical sample welded by a single pass.

As showed on the macrostructure result (figure 23) of the physical experiment, it is possible to see the characteristic “V-shape” of a GMAW welding, full penetration and apparently no defects such as cracks, porosity, inclusion, undercut or incomplete fusion. In addition, may be clearly seen the different regions affected by the heat of the welding thermal cycles that was visually eased by the bounds inserted on the image. Thus, the fusion zone (FZ) is around 4 mm on the top and decrease to approximately 2 mm on the bottom of the joint. The heat affected zone is around 3 mm and was divided by coarse grain (CGHAZ) that is located

adjacent to the fusion zone and fine grain (FGHAZ) that is located adjacent to the base material (BM).

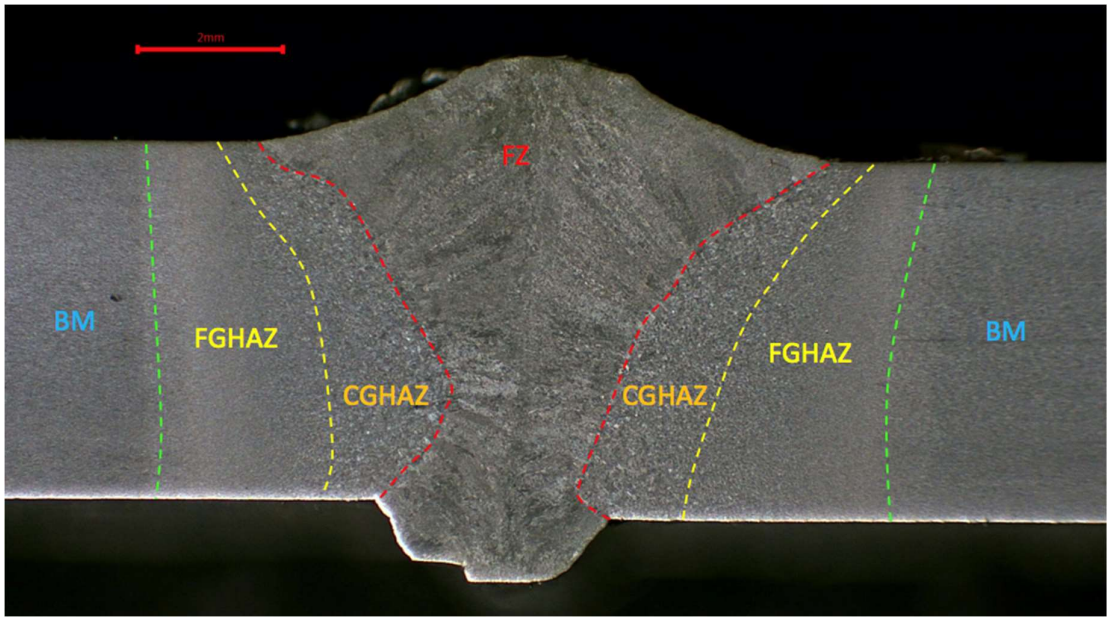

Figure 23. Macro etch cross section of a sample showing the fusion zone (FZ), coarse grain heat affected zone (CGHAZ), fine grain heat affected zone (FGHAZ) and base material (BM).

It is also important to mention that the macro etch cross section do not represents exactly a picture of the whole welding, however, it aids to obtain an overview of the general welding condition. Thus, based on the information of a visual condition as showed on the figure 23, it is possible to assume that the welding parameters considered on the analyzed material and welding process was appropriate.

4.1.2 Microhardness

The hardness results on the physical experiment are presented on the figure 24, where is also possible to visualize each region that the hardness test machine penetrated in the material (around 0.5 mm of distance from each point). The results present clearly a distinction of hardness result between the BM, HAZ and FZ. In the BM, the average hardness is around 350 HV (hardness Vickers), however, can be seen that when approximate to the HAZ, the values of the hardness tend to be lower (250 ~ 300 HV), which is a characteristic of a region

softened by a lower heat input. The only exception of the lower hardness on the HAZ is a peak hardness around 340 HV that was found exactly between the FGHAZ and CGHAZ.

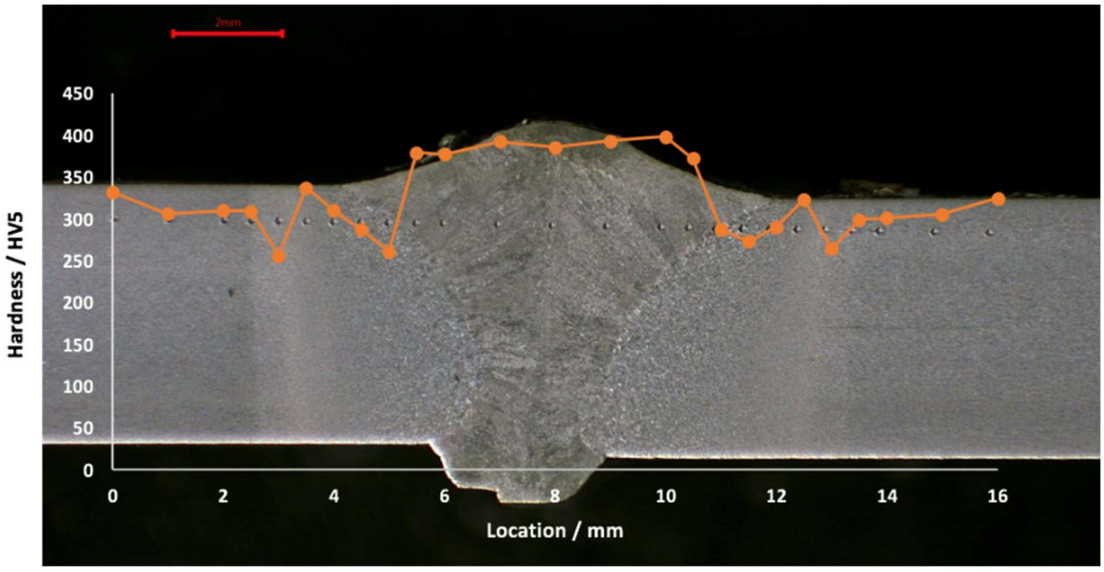

Figure 24. Hardness results (HV_5) of the experimental test.

In the other hand, the FZ showed a higher hardness value (around 400 HV), mostly due to the higher heat input in this region. If we analyze some defects that may occur on a welding joint related to the hardness, the cold cracking is an example and an alternative to mitigate this menace is control the peak hardness value on the HAZ. In this way, in steels with low carbon content (around 0.06%) the peak hardness should remain below than 350 HV. (Mohrbacher, Spöttl & Paegle 2015, p. 8.)

As mentioned, the chemical composition of the material used is totally relevant to understand the hardness results. Thus, it is essential to early evaluate the carbon content of the material to predict some effects from the welding heat input. The carbon content was also observed by O´Brien (2011, p. 17) that examined the tendency to have cracks on material with lower hardness level, which is the opposite on welding materials that have higher carbon content and are more receptive to reach higher hardness. In addition, the same 350 HV mentioned before that was considered as a reference to a boundary value, was defined as a conventional value for in-service welding, which is contrary to others non-conventional welding application.

As a complement of the results already obtained by the hardness test result, trough the analysis from the welding laboratory, it was obtained the continuous cooling transformation (CCT) diagram of unprocessed Optim® 960 QC (figure 25) that presents many relevant information of the base material under a certain temperature. Thus, it was possible to predict the microstructure phases of the material trough the cooling rate information and relate it to with the hardness. Regarding to the microstructure, could be possible to visualize that by the hardness value reached, a bainite structure was formed around a cooling rate of 40 ºC/s, which is suitable to the HAZ of the physical sample. However, to reach higher values around 400 HV on the FZ, the microstructure formed martensite and bainite structure, that is related to a cooling rate around 70 ºC/s.

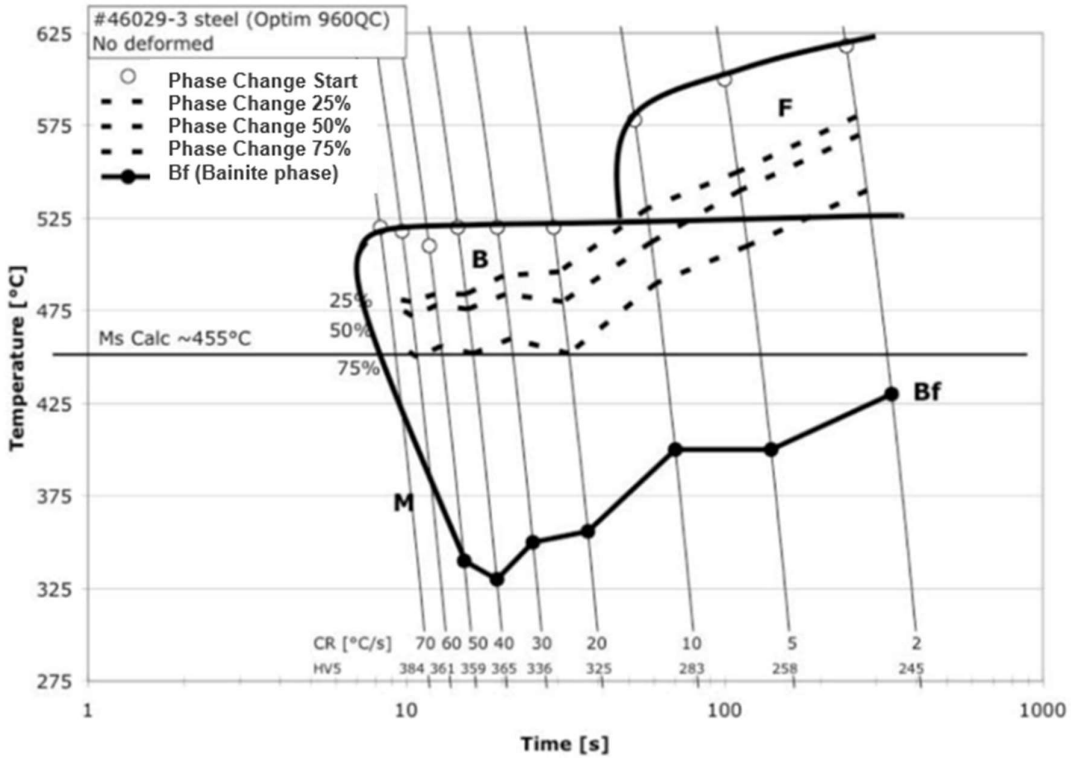

Figure 25. CCT diagram for an unprocessed Optim® 960 QC material.

The results found on CCT diagram are directly influenced by the heat input, since it is derived from the welding parameters. Subsequently, a similar material to the present research was already evaluated by Mohrbacher et. al (2015, p. 9) and it was brought a limit of 1.2 kJ/mm to the maximum heat input on GMAW process, in order to avoid softening in

the HAZ. In opposite, if considered a value under 1.0 kJ/mm, unwanted hardness peaks may should appears, which became the HAZ susceptible for cold cracking.

4.1.3 Thermal cycle by thermocouples

As presented before on the experimental procedure, it was used five thermocouples located on the top surface of the plates in order to measure the behavior of the temperature during the welding. Thus, the measured peak of temperature the thermocouple from the distance of 6.8 mm that is the closest to the centerline welding is approximately 42 ºC/s, that is well-suited to the microhardness result and its respective value of cooling rate, if the Figure 26 is considered. Remembering that to the FZ, which there was no thermocouples to evaluate, the cooling rate presented before of around 70 ºC/s is totally adequate to the CCT of the material. Thus, the cooling rate value was based on the following equation:

$$T_{800-500} = \frac{300}{\Delta t_{8-5}} \tag{3}$$

In equation 3, $T_{800\text{-}500}$ is defined as the cooling rate and $\Delta t_{8\text{-}5}$ is the difference between the initial and final time from the 800 ºC and 500 ºC, since this range is propitious to the phase transformation (Poorhaydari, K., Patchett, B. & Ivey, D. 2005, p. 154-s). The found predicted cooling time regarding to the samples was around 8.9s.

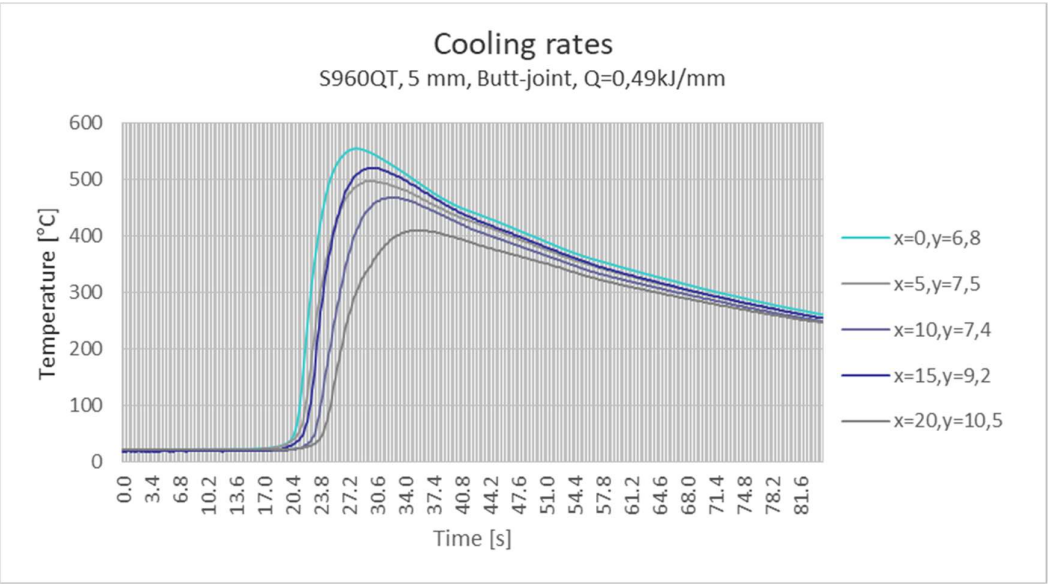

Figure 26. Thermal cycle obtained by the physical sample experiment.

In order to obtain a better understanding of the effects of the heat input on welding, the cooling rate may direct to a precise prediction of the welding, that are connected to the welding parameters. Additionally, as stated by Guo et al. (2017, p. 6), the cooling rate has an essential role on the welding through the effect on the microstructure. In addition, are known that along with the increase of the heat input, on the other hand, slower is the cooling rate, conversely.

4.2 Welding simulation results

In the present research, the purpose of the use of a computational method is to approximate to the real condition a structural and thermal behaviors evaluation of different scenarios without the necessity to produce a real specimen. The following results will present mainly different conditions of heat input, that is derived from the changes on the welding parameters and the amount of welding passes.

In the figure 27, it was considered a single pass welding at 0.49 kJ/mm of heat input, which corresponds exactly to the same value on the physical specimen. In this way, the intention to use the same condition is due to the possibility to “calibrate” the software and reproduce in other parameters without the necessity to predict a result by the welding process. As a result, it was found a similarity with the peak temperature around 550 ºC achieved on the temperature probe 1 along the physical model. The cooling rate of the same probe was approximately 47 ºC/s, which is closer to the 42 ºC/s found on the physical specimen.

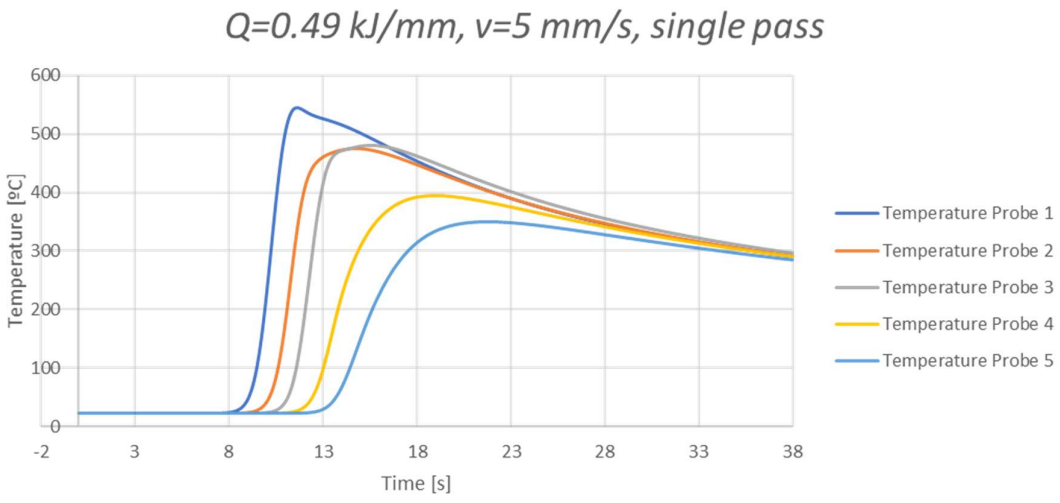

Figure 27. Thermal cycle of a single pass welding at Q=0.49 kJ/mm, v=5 mm/s.

In the figure 28, the thermal cycle shown is still related to a single pass, however, the welding parameters were changed with the intention of achieve a higher heat input of 0.84 kJ/mm than the previous test. Thus, the peak temperature of the probe 1 was around 900 ºC, which is visibly an elevated temperature if compared to the previous condition. If we focused on the microstructure, the transformation of the material in the tested heat input is estimated to be predominant bainite with a mixture of martensite, that is like to the 0.49 kJ/s heat input. This effect may be evidenced by the cooling rate of approximately 19 ºC/s, which is slower if compared to the 0.49 kJ/mm heat input used previously. Another difference between both tested results is the estimate of the hardness in approximately 325 HV, that is slight lower than what was found on the physical and virtual sample of 0.49 kJ/mm.

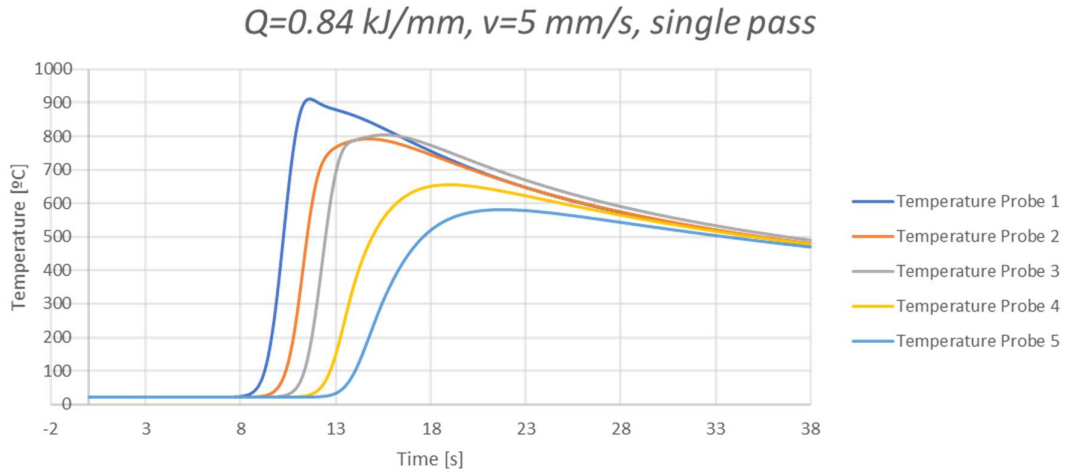

Figure 28. Thermal cycle of a single pass welding at Q=0.84 kJ/mm, v=5 mm/s.

With the aim to evaluate not only different welding parameters, but also different welding conditions, the figure 29 shows the results from the thermal cycle in a simulation of multi-pass welding, where 3 welding passes were performed. In this type of welding condition, the interpass welding is a factor that must be considered to evaluate the welding heat input. To the computational simulation, the nominal value of 0.49 kJ/mm heat input used on the physical and virtual specimen was also considered on this simulation to ease the comparison. Thus, the interpass welding simulation presented a difference of temperature from each welding pass around 200 ºC. In this way, due to the influence of the heat input in a single pass welding result of 0.84 kJ/mm, we may assume that with a high heat input, higher will be the interpass temperature.

The interpass control temperature is essential to avoid some defects on welding. As an example, Jenney & O'Brien (2001, p. 150) stated that one method to minimize intergranular corrosion on welding is maintain the interpass temperature under 121 ºC. Thus, due to different requirements, the interpass temperature must be controlled and using welding simulation, this condition may be predicted. Another consideration of the multi-pass welding is regarding to the microstructure changes, that are more influenced by the different thermal in the same structure.

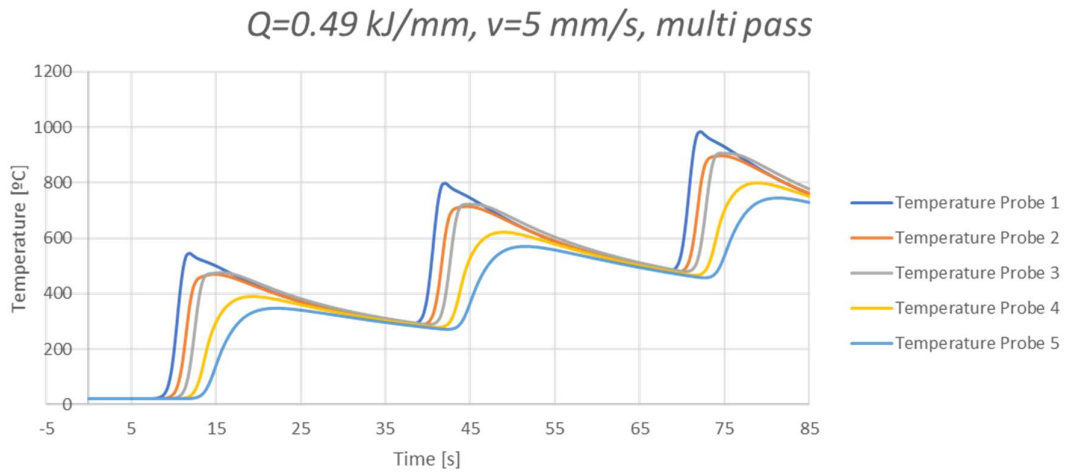

Figure 29. Thermal cycle of a multi-pass welding at Q=0.49 kJ/mm, v=5 mm/s.

An overview of the both single and multi-pass welding is showed in the figure 30. The extension of the HAZ is observed along a temperature map, where the highest temperatures are around the heat source. Base on the image of the multi-pass welding, it was clear that due to the welding passes, there is a cumulative heat input, that became wider the extension of the HAZ. In a research related to the influence of different welding input on S1100QL material, Nowacki et al. (2016, pp. 783) evidenced that with increase of heat input on the joint directed to a change in the microstructure, with a tempering martensite structure, derived from a grain growth. In addition, it was also observed that the well control of the heat input may lead to the necessary equilibrium between the weld hardening and tempering. Those methods are essential to predict a final strength result on a determined structure.

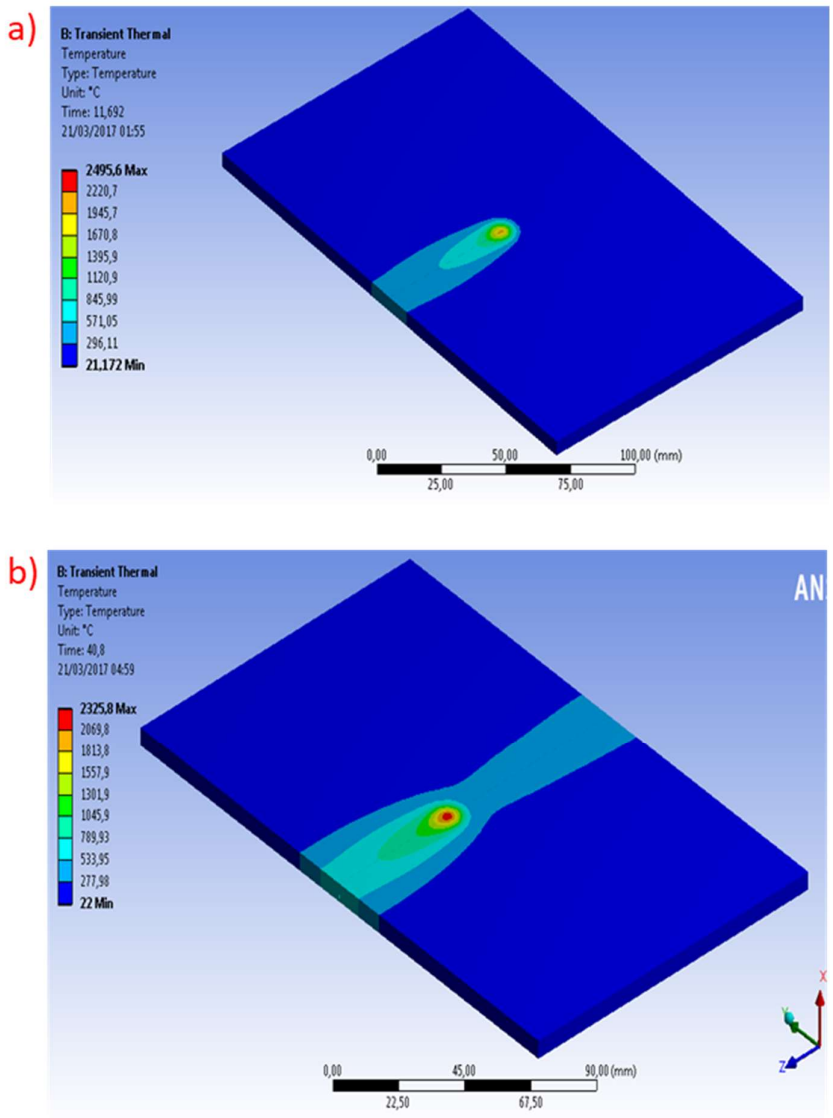

Figure 30. Temperature distribution on a welding at (a) Q=0.49 kJ/mm, v=5 mm/s, single pass and (b) Q=0.49 kJ/mm, v=5 mm/s, multi-pass.

The difference of the single and multi-pass heat input is better observed when the both cross cut sections are compared. So, the figure 31 shows a comparison between the temperature distribution on a cross section of each virtual sample, when both are Q=0.49 kJ/mm and v=5 mm/s. Accordingly, is visibly that the HAZ of the multi-pass condition is almost two times higher than the single pass. It is important to mention that the image captured from the software is related to the third pass performed on the virtual sample, to evaluate the worst condition of the heat input from a multi-pass welding.

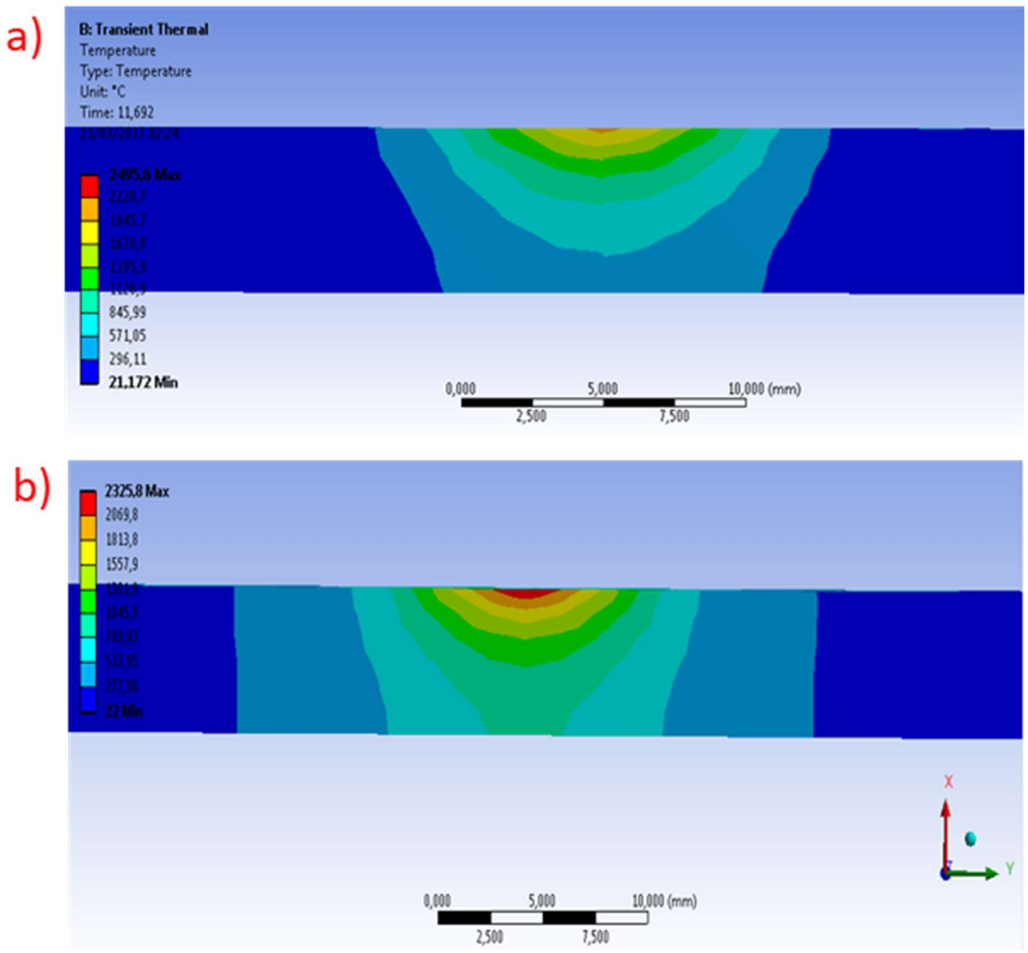

Figure 31. Temperature distribution on a cross section welding at (a) Q=0.49 kJ/mm, v=5 mm/s, single pass and (b) Q=0.49 kJ/mm, v=5 mm/s, multi-pass.

In order to validate the results obtained by the computational simulation, a transversal cut was accomplished on the virtual sample and then compared to the real specimen (figure 32). This analysis provides the possibility to estimate the extension of the HAZ based on the temperature distribution obtained. In general, as closer is the from the top surface of the plates, where the source is located, as higher and center is the temperature. In the Figure 27 is also possible to see clearly that the shape created of the GMAW process is like the found on the physical model. Hence, this shape was expected, and it emphasize the good alignment between both numerical and experimental tests.

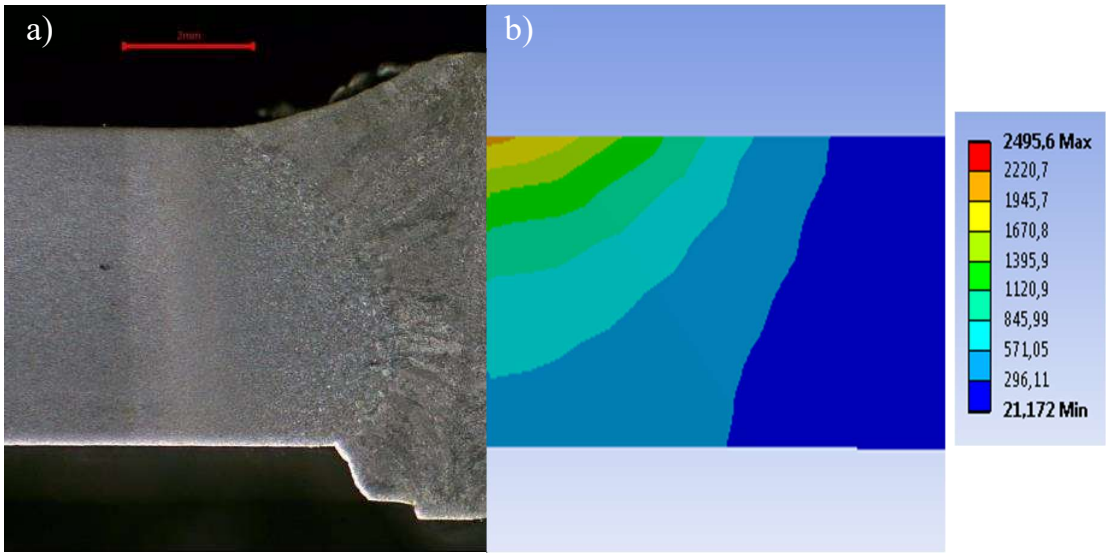

Figure 32. Comparison of the fusion zone between the physical (a) and the virtual (b) experiment.

The comparison of the fusion zone by an image for both methods is roughly demonstrated, though with the correct software resources available, the predictions may be performed by only changing welding parameters to a best fit of the real condition, giving the necessary assumptions of a real condition. Additionally, as stated by Goldak & Akhlaghi (2005, p. 119-120), a computational simulation to predict the behavior of HAZ bring many benefits, mostly due to the elevated sensitivity of the HAZ, which is also followed by the high dependency of the microstructure behavior of that region.

Since the present study focused on the heat input, it is important to relate the impact of this factor not only in the microstructure, but also in the deformation along the temperature and time. The deformation was not measured on the physical specimen, so, it was not possible to be compared. The thermo-mechanical characteristics were evaluated by the same software used on the thermal analysis, though, it was used another module to insert the information already collected from the thermal analysis on a thermo-mechanical evaluation. The intent to present this result is to exemplify another feature available that aids to predict the behavior of a certain welding parameter. Thus, in the figure 33, the equivalent stress shows the critical regions and the peak of the sample, where the stress has more impact. This type of analysis is essential during the development a welded structure, since allows to evaluate an assembly where many parts are involved, and a part stress result may influentiate in the failure of the whole structure.

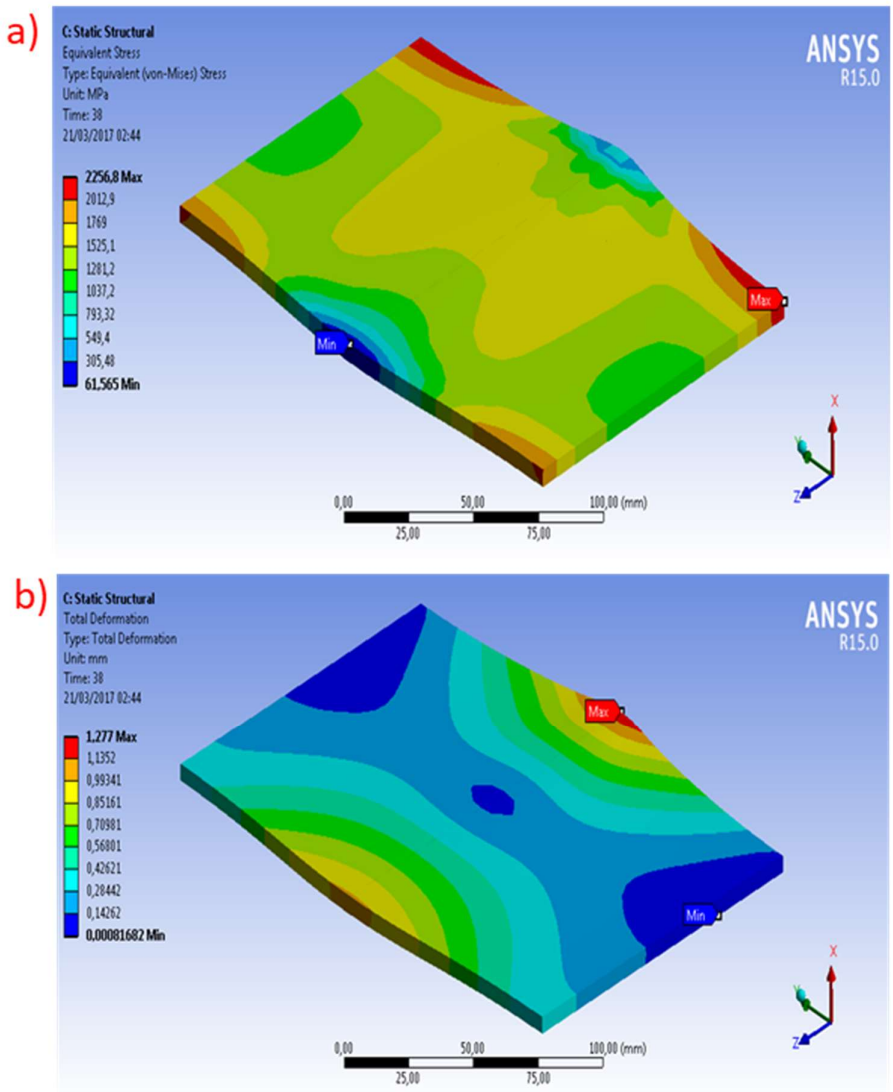

Figure 33. Equivalent stress (a) and total deformation (b) on a welding at Q=0.49 kJ/mm, v=5 mm/s, single pass.

At last, the total deformation is also presented with the aim to present the variation in mm of the single pass condition of a welding at Q=0.49 kJ/mm. During the experimental test, it was noticed that the gap air had a variation from 0 to 0.5, which is mostly due to a natural condition of deformation. Though, the results from the computational method presents a 1.277 mm that is suitable to the real condition deformation found. Once more, this type of condition eases the design of structure, parts or other welded assembly to ensure that all the aspects influenced by the heat input are covered during the development.

5 CONCLUSION AND SUMMARY

The most important and notable statement of this thesis are the great effect of heat input on UHSSs and the different methods that can be used to predict its impact. Since the methods considerate on this research had been already used in other materials, the focus of the research was related to the UHSSs and its sensitive characteristic. Answering the research questions, either by considering a physical experiment or a computational simulation, it was possible to evidence that the welding parameters (current, voltage, welding speed, among others) has a direct impact on the heat input. Furthermore, based on the results found, the GMAW process was suitable to weld the UHSSs. However, due to the elevated heat input of this welding process, is important to considerate a welding features that may control or provide a lower heat input, such as laser or pulse welding.

The prediction of the behavior of the welding could be accomplished not only by equations, but also using the computational welding simulation. By using the FEA, it was possible to estimate the extension of the HAZ, and then predict the result of the welding and its impact on the microstructure. The cooling time is a variable that may be predicted and could be noticed the gain of consider a range until 15s on UHSSs materials. Additionally, to obtain a high quality and reliable welding, the weld pool size and shape has a considerable influence to achieve a satisfactory result, thus, the joint also requires a special consideration, since the lower of volume melted, lower is the amount of heat. The recommended heat input will vary from the thickness of the material, nevertheless, to this study, was shown that the heat input of 0.49 kJ/mm was appropriate to the 5 mm thickness plate.

Another important result found was the influence of a cumulative heat input on joints through multi pass welding, which has a greater effect on the microstructure of UHSSs if compared to a single pass welding joint. In this way, before to predict a result, an alternative is to change the design of a structure to avoid multi passes. Moreover, the UHSS proposal also bring alternative solutions as well as the use of this material has the aim to reduce the thickness of structures through its strength benefits, which consequently may reduce the amount of welding passes. Besides, another advantage of the computational analysis is based on the interactivity of different interfaces that may predict not only the heat input effect but

also the impact of the welding by its distortion and shrinkage consequence. Accordingly, the peak temperatures obtained initially may be used as an input to evaluate the thermo-mechanical effects.

At last, the utilization of UHSS and its benefits to a welded structure has been demonstrated as a suitable choice offering a great versatility by the use on different applications. Furthermore, could be easily noticed the improvements that this new generation has obtained, and this research could evidence that is possible to achieve results with excellence on welded structures made with UHSSs. However, a challenge on welding UHSSs consists on the several range of materials and grades with different heat treatments and alloys, which to the welding process, may bring difficulty to precisely predict without an early analysis. Moreover, as well as the most of the prediction's methods, the computational welding simulation approximates a real condition and must be faced as a tool that will never replace the reality but aids to support a decision making.

5.1 Reliability, validity and error analysis of the study

Besides the triangulation method with the aim to ensure the reliability of the research, some steps were taken in consideration. In this way, the necessary information to conduct both the experimental and virtual tests were collected from reliable sources. The technical resources from the material used was provided by the manufacturer. The equipment's used during the tests were calibrated and the comparison between the virtual specimen with the physical along adjustments, aided to guarantee the reliability.

However, even using as input in the FEA information that are coming from reliable sources, this analysis method is also a possible source of error, due to the differences between models based on a numerical behavior. Another possible source of errors is the comparison of equations with some diagrams and graphs presented, since it is an approximation and may carry a slight error when it is used to compare.

The validity of this research it was appropriate, since the results obtained were compared with other research results and even other results were used as reference to understand the behavior of the present research. Besides to compare the results, another aspect is the qualitatively and quantitatively comparison between the results and the researches.

However, in the time that a small quantity of laboratory test specimen was considered, this is an indicator of an eventual error analysis, in other hand, to achieve a satisfactory result, is not necessarily a statistical study that may lead to adequate study.

5.2 Further studies

The welding process has a main role in the production and technology of many sectors and the development of this process along new generations of materials has increased proportionally. As a challenge, the welding process should also be increasingly intelligent and reliable, to predict different results inherent of the many existing variables. Thus, this study brought different possibilities to consider welding parameters and even the material used in the analysis of a specific welding process, however, as a portion of a wide field, there are other subjects that need to be added in a future research. In this way, follow below some topics that may be further studied along with the present study:

1. Reproduce the present research with different grades of UHSS and/or welding parameters:
    a. Since it was used a specific grade of UHSS, it would be essential to reproduce the methodology adopted on this research along with other grades. It is also important to remember that the grades of AHSS and UHSS are constantly in development, which fortify the necessity to reproduce the present study with other material grade;
2. Intelligent control using Artificial Neural Network (ANN):
    a. The computational models based on ANN in the welding are an interesting approach to optimize the process based on the variables that may be controlled during the execution of the welding process. Welding variables such as welding speed, arc voltage and current are examples of what can be used as an initial input and then controlled to predict a desired result. In this way, to use these models on the welding are in the same time a challenge, but also a encourage approach.
3. Real-time monitoring:
    a. Due to the significance of the heat in the welding of UHSS, the utilization of accurate cameras and sensors that may monitor the temperature and the images of the welding on real-time are another opportunity to utilize a

different method in the future. In addition, the computed information may be used as an input to the ANN mentioned previously.

REFERENCES

3rd-generation Advanced High-strength Steel. 2013. Tribology & Lubrication Technology, vol. 69, no. 2. pp. 10-11.

Abraham, A. 2015. Metallic Material Trends in the North American Light Vehicle [web document]. May 2015 [Referred 10.11.2016]. Ducker Worldwide & Auto Steel Presentation. Great Designs in Steel Seminar. 21 p. Available in PDF File: http://www.autosteel.org/~/media/Files/Autosteel/Great%20Designs%20in%20Steel/GDIS%202015/Track%202%20-%20Abraham.pdf.

Alriksson, S. & Henningsson, M. 2015. Why Aren't Advanced High–Strength Steels More Widely Used?: Stakeholder Preferences and Perceived Barriers to New Materials. Journal of Industrial Ecology, vol. 19, no. 4. pp. 645–655.

ANSYS. 2016. Moving Heat Source. [ANSYS Customer Portal]. Updated February 26, 2016 [Referred 10.10.2017] Available: https://appstore.ansys.com/download?prodid=APC-ACTAPP-105

Aydin, H., Essadiqi, E., Jung, I. & Yue, S. 2013. Development of 3rd generation AHSS with medium Mn content alloying compositions. Materials Science and Engineering: A, vol. 564, 1 March. pp. 501-508.

Bhatti, A., Barsoum, Z., Murakawa, H. & Barsoum, I. 2015. Influence of thermo-mechanical material properties of different steel grades on welding residual stresses and angular distortion. Materials & Design, vol. 65. pp. 878–889.

Böhler Welding. 2014. Böhler Welding Products. [Voestalpine webpage]. Updated December 2014 [Referred 28.03.2017] Available: http://www.vabw-service.com/documents/boehler/datenblaetter/en/T_Union%20X%2096_de_en_5.pdf?cache=1505664871

Bozickovic, Z., Maric, B., Dobras, D., Lakic-Globocki, G. & Cica, D. 2015. Virtual Modeling of Assembly and Working Elements of Horizontal Hydraulic Press. Annals of the Faculty of Engineering Hunedoara, vol. 13, no. 3. pp. 165-168.

Demeri, M. Y. 2013, Advanced High-Strength Steels: Science, Technology, and Applications. Ohio: ASM International. 301 p.

Fonstein, N. 2015. Advanced High Strength Sheet Steels: Physical Metallurgy, Design, Processing and Properties. Switzerland: Springer International. 396 p.

Ford Motor Company. 2011. Ultra-High Strength Steels: Enhancing vehicle safety and improving fuel efficiency [Ford Motor Company webpage]. Updated July 2011 [Referred 23.01.2017]. Available: https://media.ford.com/content/fordmedia/fna/us/en/asset.download.document.pdf.html/content/dam/fordmedia/North%20America/US/2013/07/19/Safe/Boron.pdf.

Goldak, J. & Akhlaghi, M. 2005. Computational Welding Mechanics. New York: Springer. 321 p.

Guo, W., Crowther, D., Francis, J., Thompson, A., Liu, Z. & Li, L. 2015. Microstructure and mechanical properties of laser welded S960 high strength steel. Materials & Design, vol. 85. pp. 534–548.

Guo, W., Li, L., Dong, S., Crowther, D. & Thompson, A. 2017. Comparison of microstructure and mechanical properties of ultra-narrow gap laser and gas-metal-arc welded S960 high strength steel. Optics and Lasers in Engineering, vol. 91. pp. 1–15.

Jeffus, L. 2012. Welding: Principles and Applications. Seventh edition. New York: Delmar Cengage Learning. 947 p.

Jenney, C. & O'Brien, A. 2001. Welding Handbook: Welding Science and Technology. Ninth edition. Volume I. Miami: American Welding Society. 872 p.

Kou, S. 2003. Welding Metallurgy. Second edition. New Jersey: John Wiley & Sons Inc. 461 p.

Krasovskyy, A. & Virta, A. 2015. Fatigue life assessment of welded structures based on fracture mechanics. International Journal of Structural Integrity, vol. 6, no. 1. pp. 2-25.

Laitinen, R., Valkonen, I. & Kömi, J. 2013, Influence of the base Material Strength and Edge Preparation on the Fatigue Strength of the Structures Made by High and Ultra-high Strength Steels. Procedia Engineering, vol. 66, pp. 282–291.

Májlinger, K., Kalácska, E. & Spena, P. 2016. Gas metal arc welding of dissimilar AHSS sheets. Materials & Design, vol. 109. pp. 615–621.

Martis, C. J., Putatunda S. K. & Boileau J. 2013. Processing of a new high strength high toughness steel with duplex microstructure (Ferrite + Austenite). Materials & Design, vol. 46, April. pp. 168-174.

McCallion, R. 2012. Manufacturing with UHSS [Automotive Manufacturing Solutions webpage]. Updated July 1, 2012 [Referred 05.07.2016]. Available: http://www.automotivemanufacturingsolutions.com/process-materials/manufacturing-with-uhss.

Mohrbacher, H., Spöttl, M. & Paegle, J. 2015. Innovative manufacturing technology enabling light weighting with steel in commercial vehicles. Advances in Manufacturing, vol. 3, no. 1. pp. 3-18.

Neimitz, A., Dzioba, I. & Limnell, T. 2012. Modified master curve of ultra-high strength steel. International Journal of Pressure Vessels and Piping, vol. 92, pp. 19–26.

Nowacki, J., Sajek, A. & Matkowski, P. 2016. The influence of welding heat input on the microstructure of joints of S1100QL steel in one-pass welding. Archives of Civil and Mechanical Engineering, vol. 16, no. 4, pp. 777–783.

O'Brien, A. 2004. Welding Handbook: Welding Processes, Part 1. Ninth edition. Volume II. Miami: American Welding Society. 720 p.

O'Brien, A. 2011. Welding Handbook: Materials and Applications, Part 1. Ninth edition. Volume IV. Miami: American Welding Society. 695 p.

Perret, W., Thater, R., Alber, U., Schwenk, C. & Rethmeier, M. 2011. Approach to assess a fast welding simulation in an industrial environment – Application for an automotive welded part. International Journal of Automotive Technology, vol. 12, no. 6. pp. 895-901.

Poorhaydari, K., Patchett, B. & Ivey, D. 2005. Estimation of cooling rate in the welding of plates with intermediate thickness. Welding Journal, 84. pp. 149-s.

Qiang, X., Jiang, X., Bijlaard, F. & Kolstein, H. 2016. Mechanical properties and design recommendations of very high strength steel S960 in fire. Engineering Structures, vol. 112, pp. 60–70.

Ramazani, A. et al. 2014. Micro–macro-characterisation and modelling of mechanical properties of gas metal arc welded (GMAW) DP600 steel. Materials Science and Engineering: A, vol. 589. pp. 1–14.

Ruuki. 2010. Technological Properties of Direct-quenched Structural Steels with Yield Strengths 900-960 MPa as Cut Lengths and Hollow Sections. [Oxycoupage webpage]. Updated 2010 [Referred 30.03.2017]. Available: http://oxycoupage.com/FichiersPDF/Ruukki_Pdf/English/Ruukki-Technical-article-Technological-properties-of-direct-quenched-structural-steels.pdf

Shome, M. & Tumuluru, M. 2015. Welding and Joining of Advance High Strength Steels (AHSS). Cambridge, UK: Woodhead Publishing. 204 p.

Van Rensselar, J. 2011. The riddle of steel: A-UHSS. Tribology & Lubrication Technology, vol. 67, no. 7. pp. 38-40, 42-46.

World Auto Steel. 2014. Advanced High-strength steels application guidelines version 5.0. [World Auto Steel webpage]. Updated May 2014 [Referred 01.11.2016]. Available: http://www.worldautosteel.org/downloads/advanced-high-strength-steels-application-guidelines-v5/

World Auto Steel. 2017. Advanced High-strength steels application guidelines version 6.0. [World Auto Steel webpage]. Updated April 2017 [Referred 03.08.2017]. Available: http://www.worldautosteel.org/projects/advanced-high-strength-steel-application-guidelines/

Material certificate of the material used in the experimental test.

RUUKKI

AINESTODISTUS TEST REPORT
WERKSZEUGNIS RELEVE DE CONTROLE
EN 10 204-3.1 (2004)

B 8/10
39859 -01

Tilaaja Purchaser Besteller Acheteur
RAUTARUUKKI OYJ
RUUKKI PRODUCTION
Tilaus nro Order No. Bestellung Nr. Commande No.

Vastaanottaja Consignee Empfänger Destinataire
LAPPEENRANNAN TEKNILLINEN
YLIOPISTO
Läh. merkki Shipping mark Versandzeichen Marque d'expedition

Päivämäärä Date Datum Date
28.03.2006
Valmistajan merkki
Mark of the Manufacturer
Zeichen des
Herstellerwerkes
Signe de producteur

Laatu Quality Werkstoff Nuance
OPTIM 960 QC
Laatuselvitys Quality Specifications Qualitätspezifikation Spécification de qualité
MUOVATTAVA LUJA TERÄS

Lisävaat. Add. requirem. Weitere Anforder Autres prescript.
OPTIM, EN 10051

Jatkuvavalettua
happiterästä
Oxygen steel,
continuous casting
Oxygenstahl, Stranggus
Acier a l'oxygene,
coulée continue

Positio Item Pos. Poste	Paksuus Thickness Dicke Epaiss.	Sulatus nro Cast No Schmelz-Nr. No coulée	Cekv Ceq Cäq Cég	Sulatusanalyysi % Chemical composition of cast % Chem. Zusammensetzung auf schmelzen % Composition Chimique de coulée %												
				C	SI	MN	P	S	AL	NB	V	TI	CU	CR	NI	MO	B
001	4.00	85773	.47	.09	.19	1.07	.009	.002	.033	.003	.006	.022	.029	0.83	0.04	.160	.0021
002	5.00	85775	.46	.09	.21	1.05	.010	.004	.030	.003	.008	.032	.025	0.82	0.04	.158	.0019
003	6.00	85775	.46	.09	.21	1.05	.010	.004	.030	.003	.008	.032	.025	0.82	0.04	.158	.0019

CEKV=C+MN/6+(CR+MO+V)/5+(NI+CU)/15

Pos. Item Pos. Poste	Sulatus, k.erä nro Cast, test No Schmelze Prüf Nr. Coulée, Essai No	T-tila Cond Zust. Etat	Vetokoe, Tensile test Zugversuch, Essai de traction			Taivutusk Bend test Faltvers. Edepliage D = X t	Iskukoe, Impact test Kerbschlagversuch, Essai de retilience						Erikoiskokeet Special tests Sonderversuche Essais Speciaux	
			K2	Re N/mm2	Rm N/mm2	A %	K3	°C	1	2	3	Keskiarvo Average Mittelw. Moyenne		
				RP02 REH		5							RP0.2	RM N/MM2
001	85773 031	Q	32			11	*7.0						1040	1125
002	85775 032	Q	32			12	*7.0	137	-40	068	089	065	074	976	1108
								138	-40	060	060	057	059		
003	85775 041	Q	32			11	*7.0	137	-40	086	086	086	086	969	1104
								138	-40	058	074	072	068		

*: 7.0=120 MM LEVEÄ SÄRMÄYSKOE
K2: 32=KESKELTÄ, PITKITT.
K3: 137=CH-V(J),TX10,KESKELTÄ,PITKITT., 138=CH-V(J),TX10,KESKELTÄ,POIKITT.

RUUKKI PRODUCTION
Raahe Steel Works
Testaus ja tarkastus Testing and Inspection
Prüfung und Kontrolle Essais et Contrôle

Täten todistamme, että toimitus on tilausvahvistuksen mukainen.
We hereby certify that the material described above has been tested and complies with the terms of the order contract.
Es wird bestätigt, dass die Lieferung geprüft wurde und den Vereinbarungen bei der Bestellannahme entspricht.
Nous certifions que la livraison est conforme aux stipulations de l'acception de la commande.

30.03.2006 MLS

MINNA VALKAMA
Valtuutettu tarkastaja Authorized Inspector Puh. 020 5911
Werksachverständiger Inspecteur autorisé Tel. +358 20 5911

RTC97

AR kuumavalssattu as rolled
N normalisoitu normalized
NR normalisointi valssattu normalizing rolling
CR kontrolloiduisti valssattu controlled rolled
TM termomek valssattu thermomech. treated
QT karkaisu + päästö quenched + tempered
Q karkaistu quenched